Thesis

On

EVALUATION OF MECHANICAL BEHAVIOUR OF FRICTION STIR WELDED JOINTS

Submitted in partial fulfillment of the requirement for the award of the degree of

Master of Engineering

IN

PRODUCTION & INDUSTRIAL

Submitted By

PRITIKA PATHAK

Roll No. 800982018

Under the Guidance of:
Dr. S.K. Mohapatra
Dean of Academic Affairs,
Thapar University,
Patiala-147004

DEPARTMENT OF MECHANICAL ENGINEERING
THAPAR UNIVERSITY
PATIALA-147004, INDIA
JUNE-2011

DECLARATION

I hereby declare that this thesis entitled "**EVALUATION OF MECHANICAL BEHAVIOUR OF FRICTION STIR WELDED JOINTS"** is an authentic record of my study carried out as requirements for the award of the degree of **Master of Engineering (Production and Industrial)** at **Thapar University, Patiala**, under the guidance of **Dr. S.K. Mohapatra,** Dean of Academic Affairs, Thapar University, Patiala, during July 2010 to June 2011.

The matter embodied in this report has not been submitted in part or full to any other university or institute for the award of any degree.

Dated: **(Pritika Pathak)**

This is to certify that above declaration made by the student concerned is correct to the best of my knowledge & belief.

Dr. S.K. Mohapatra
Senior Professor in Mechanical Engineering
Dean of Academic Affairs
Thapar University, Patiala-147004

(Counter signed by)

Dr. Ajay Batish
Professor and Head
Department of Mechanical Engineering
Thapar University,
Patiala-147004

Dr. S.K. Mohapatra
Dean of Academic Affairs
Thapar University,
Patiala-147004

ACKNOWLEDGEMENT

My foremost and profound gratitude goes to my supervisor Dr. S.K. Mohapatra for his proficient and enthusiastic guidance and encouragement. The suggestions given by him undoubtedly helped in supplementing my thoughts in the right direction for attaining the desired objective.

I would like to express a deep sense of gratitude and thank profusely to Dr. Rahul Chhibber for his sincere & invaluable guidance.

My heartfelt gratitude goes to Dr. Ajay Batish, Prof. & Head, HMED for providing all the facilities required for the completion of my work.

I would like to thank the non teaching staff, Mr. Rajinder Kumar, Mr. Narinder, Mr.R.K. Banerjee, Mr. A.S. Cheema and all the workshop staff who helped me in various aspects of my research.

I am very much thankful to members and employees of Mechanical Department, TU, Patiala for who have contributed directly or indirectly towards the successful completion of my thesis work on time. All above, I express my indebtedness to thee "ALMIGHTY" for all His blessings and kindness.

Pritika Pathak

Registration N0:800982018

ABSTRACT

Friction stir welding is a solid state joining technique that is widely being used for joining aluminium alloys in industries, especially the shipbuilding, aerospace, mass transportation and automotive and many other applications of commercial importance. This process is considered as a **"green technology"** due to its energy efficiency, environmental friendliness, and versatility. Friction stir welding was carried out using a vertical milling machine on Aluminium 6063 alloy. The tool material and geometry were carefully chosen and prepared using lathe machine. Important process parameters that control the quality of the weld are rotation speed (rpm), traverse speed (mm/min), tool depth (mm) and tool tilt angle and these process parameters were optimized to obtain defect free welded joints. It is observed that, during the friction stir welding, extensive deformation takes place at the nugget zone and the evolved microstructure that strongly affects the mechanical properties of the joint. The aim of present study is to understand the mechanical properties and micro structural changes of the friction stir welded joints.

CONTENTS

LIST OF TABLES

LIST OF FIGURES

ABBREVATIONS

FSW	Friction stir welding
AA6063	Aluminium Alloy 6063
HAZ	Heat Affected Zone
TMAZ	Thermo mechanically Affected Zone
PCBN	Polly Crystalline Boron Nitride
CBN	Cubic Boron Nitride

CHAPTER 1

FRICTION STIR WELDING - AN OVERVIEW

1.1 INTRODUCTION

Friction Stir Welding (FSW) was invented by The Welding Institute (TWI) of the United Kingdom in 1991 as a solid-state joining technique and was initially applied to Aluminium alloys and is extensively used in joining of Al, Mg, Cu, Ti and their alloys. The basic concept of FSW is that a non consumable rotating tool with especially designed pin and shoulder is inserted into the abutting edges of sheets or plates to be joined and subsequently traversed along the joint line. [1]

Friction Stir Welding is a solid state thermo mechanical joining that transforms the metal from a solid state into a ***'plastic like state'*** and then mechanically stirs the material under pressure to form a welded joint.[2] It uses a rotating non-consumable tool with shoulder and a threaded pin (Fig.1.1). The pin is slightly shorter than the thickness of the work-piece and its diameter is slightly larger than the thickness of the work-piece.

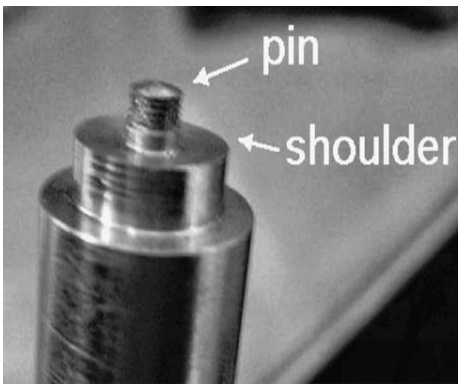

Figure.1.1: Schematic of FSW Tool [1]

In FSW, a cylindrical-shouldered tool, with a profiled threaded/unthreaded probe or pin is rotated at a constant speed and fed at a constant traverse rate into the joint line between two pieces of sheet or plate material, which are butted together as shown in Figure 1.2. The parts have to be clamped rigidly onto a backing bar in a manner that prevents the abutting joint faces from being forced apart. The length of the pin is slightly less than the weld depth required and the tool shoulder should be in intimate contact with the work piece surface. The pin is then moved against the work piece.

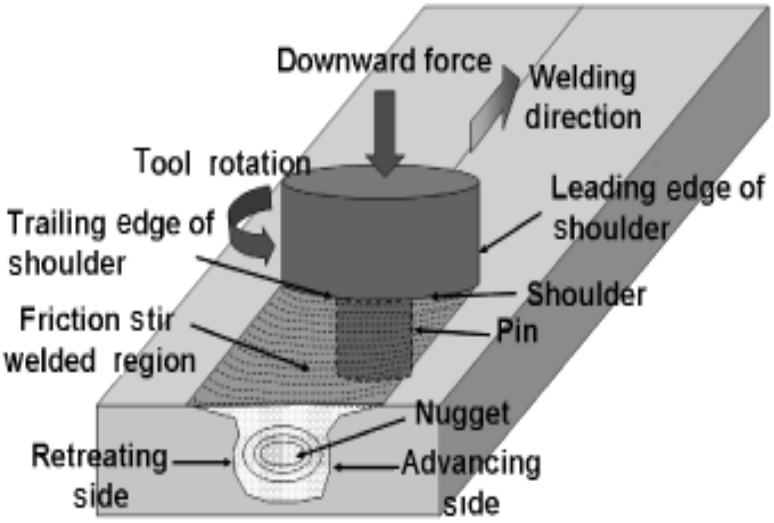

Figure1.2: Schematic of Friction stir welding [2]

The half-plate where the direction of tool rotation is the same as that of welding is called the ***advancing side***, with the other side designated as being the ***retreating side***. (Fig1.3).The advancing side is on the right, where the tool rotation direction is same as the tool travel direction (opposite the direction of metal flow), and the retreating side is on the left, where the tool rotation is opposite the tool travel direction (parallel to the direction of metal flow).

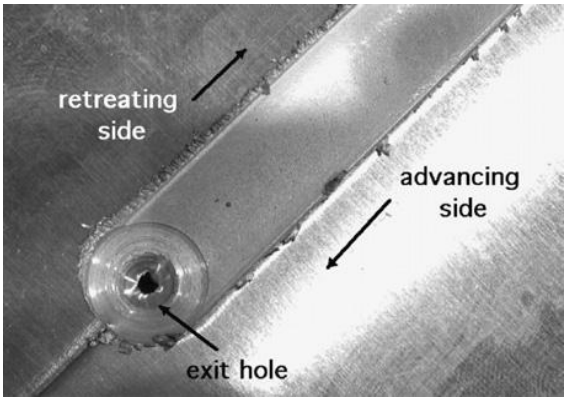

Figure 1.3: Schematic of two sides of Friction Stir Welds [2]

Friction string tool serves three primary functions ie:

1. Heating the workpiece.
2. Movement of material to produce the joint and
3. Containment of hot metal beneath the tool shoulder.

Frictional heating is created within the workpiece both by friction between the rotating pin and shoulder and by the severe plastic deformation of the work piece. This heat, along with the heat generated by the mechanical mixing process and the adiabatic heat within the material, cause the stirred materials to soften without reaching the melting point (hence cited a solid-state process).

As the pin moves in the direction of welding the leading face of the pin, assisted by a special pin profile leads to movement of plasticized material from the front to back of the pin, thus filling the hole in the plates as the tool moves forward. The tool shoulder restricts metal flow to a level equivalent to the shoulder position, that is, approximately to the initial workpiece top surface and applying a substantial force to consolidate the weld metal.

During all these operations there are no welding fumes, radiations, high voltage, liquid metals, or arcing, porosity, cracking in weld region .

A ***traditional fusion welding*** depends upon several parameters like purge gas, voltage, amperage, wire feed, travel speed, shield gas and arc gap, while the Friction stir welding process can be controlled with only few variables such as rotation speed, travel speed, tool tilt and eventually other minor variables.

This feature of the FSW proved an enhancement of the fatigue behavior and strength of the joints, leading some companies to adopt the process for the manufacturing of airplanes fuselages and cryogenic tanks for Space launch vehicles.

FSW can be used to join most Al alloys as the surface oxide is not formed and therefore no particular cleaning operation is needed prior to welding. Thus, FSW is considered to be the most remarkable and potentially useful welding technique for several materials, such as Aluminum-alloys, Magnesium-alloys, brasses, Titanium-alloys, and steels.[3,4]

1.2 PHASES OF FRICTION STIR WELDING

The FSW process can be described in the following four steps with the help of fig 1.4:

STEP 1: Start of joining/ Start by Rotating Tool:

The plates of required thickness that are to be welded are clamped together between the two jaws of the vertical milling machine with supporting plate (wood). Tool pin is clamped firmly and rotated on the top surface of the joining line of the plates.

STEP 2: Create Friction/ Starting at Edge:

Rotating pin is pushed into the material under shoulder meets the workpiece surface after a while this causes the material to plasticize due to heating by frictional contact between the tool shoulder and the workpiece.

STEP 3: Joining/ Move Tool When Metal Softens:

Tool is subsequently traversed along the joining line, it stirs the plasticized material, creating a forged weld.

STEP 4: Finished/ Pull away the Joining tool:

Process is finished when the tool is retraced from the work piece; a hole remains in the workpiece.

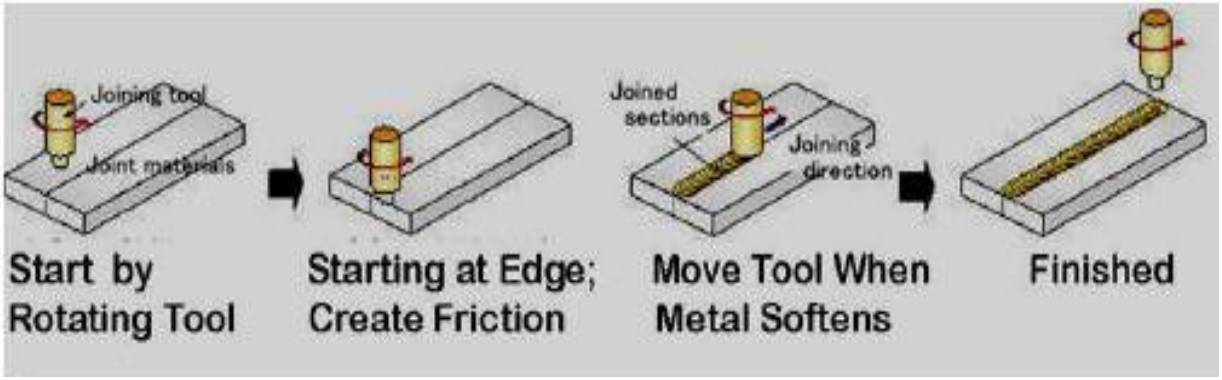

Figure 1.4: Four Steps of Friction Stir Welding Process [5]

Two plates or sheets with same thickness are placed on a backing plate and clamped firmly to prevent the abutting joint faces from being forced apart. The backing plate is required to resist the normal forces associated with FSW and the workpiece. During the initial tool plunge, lateral forces are also fairly large and extra care is required to ensure the plates in the butt configuration do not separate. To accomplish the weld, the rotating tool is plunged into the joint line and traversed along this line, while the shoulder of the tool is maintained in intimate contact with the plate surface. Tool position and penetration depth are maintained by either position control or control of the applied normal force.

1.3. DIFFERENT ZONES IN FRICTION STIR WELDING

Although tool design, speed of rotation and the material being joined can change the microstructure of a friction stir weld, yet most welds can be characterized using four

distinct micro structural zones existing after FSW [2, 7] are shown below (Fig 1.5)

Figure 1.5: Transverse section of a friction stir weld showing different regions of the weld. [2]

1. Unaffected Zone:

The zone is remote from weld that has not been deformed, although it may have experienced thermal cycle from the weld, but it is not affected by the heat in terms of microstructure or mechanical properties. The material of this zone is known as unaffected material or parent material.

2. The stir zone (also nugget, dynamically recrystallised zone):

This is the fully recrystallized area is known as stir zone refers to zone previously occupied by tool pin. It is a region of heavily deformed material that roughly corresponds to the location of the pin during welding. The grains within the stir zone are roughly equiaxed and often an order of magnitude smaller than the grains in the parent material. A unique feature of the stir zone is the common occurrence of several concentric rings which has been referred to an **'onion-ring'** structure.[6]

3. The thermo-mechanically affected zone (TMAZ) :

In this region the FSW tool has plastically deformed the material, and the heat from the process will also have exerted some influence on the material. This zone occurs on either side of the stir zone. In this region the strain and temperature are lower and the effect of welding on the microstructure is correspondingly smaller.

4. The heat-affected zone:

In this region, which lies closer to the weld-center, the material has experienced a thermal cycle that has modified the microstructure and/or the mechanical properties. However, there is no plastic deformation occurring in this area.

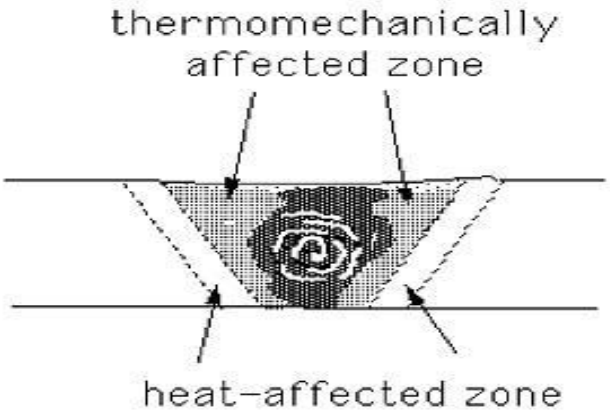

Fig 1.6: Schematic diagram of different zones of Friction Stir Weld [8]

1.4 WELDING PARAMETERS

Following are the important welding process parameters that control the quality of the weld:

1.4.1. Tool Material and Design

The design of the tool is a critical factor as a good tool can improve both the quality of the weld and the maximum possible welding speed.

It is desirable that the tool material is sufficiently strong, tough and hard wearing, at the welding temperature. Further it should have a good oxidation resistance and a low thermal conductivity to minimize heat loss and thermal damage to the machinery. Hot-worked tool steel such as AISI H13 has proven perfectly acceptable for welding aluminum alloys within thickness ranges of 0.5 – 50 mm. but more advanced tool materials are necessary for more demanding applications such as highly abrasive metal matrix composites or higher melting point materials such as steel or titanium.[9]

The tool has a circular section except at the end where there is a threaded probe, the junction between the cylindrical portion and the probe is known as the ***shoulder.*** The majority of tools have a concave shoulder profile which acts as an escape volume for the material displaced by the pin, and prevents material from extruding out of the sides of the shoulder and maintains downwards pressure and hence good forging of the material behind the tool.

The probe penetrates the workpiece whereas the shoulder rubs with the top surface. The heat is generated primarily by friction between a rotating-translating tool, the shoulder of which rubs against the work piece.

1.4.2 Tool Rotation and Traverse Speed

There are basically two tool speeds to be considered in friction-stir welding i.e

i. How fast the tool rotates-Tool rotation.
ii. How quickly tool traverses the interface.-Traverse speed

These two parameters are important for successful and efficient welding cycle. Increasing the rotation speed or decreasing the traverse speed will result in a hotter weld. In order to produce a successful weld it is necessary that the material surrounding the tool is hot enough to enable the extensive plastic flow required and minimize the forces acting on the tool. If the material is too cool then voids or other flaws may be present in the stir zone and in extreme cases the tool may break.

1.4.3 Tool Tilt and Plunge Depth

The plunge depth is defined as the depth of the lowest point of the shoulder below the surface of the welded plate. Plunging the shoulder below the plate surface increases the pressure below the tool and helps ensure adequate forging of the material at the rear of the tool.

Tilting the tool by 2-4 degrees, such that the rear of the tool is lower than the front, is also important in forging process.

The plunge depth needs to be correctly set, both to ensure the necessary downward pressure and to ensure that the tool fully penetrates the weld. Given the high loads required the welding machine may deflect and so reduce the plunge depth compared to the nominal setting, which may result in flaws in the weld. On the other hand an excessive plunge depth may result in the pin rubbing on the backing plate surface or a significant under match of the weld thickness compared to the base material.[10]

1.5 TOOL MATERIAL SELECTION

Selecting the correct tool material requires knowing which material characteristics are important for each friction stir application. Many different material characteristics [11, 12] could be considered important to friction stir welding, some of which are**:**

1.5.1 Ambient and elevated temperature strength:

The candidate tool must withstand the compressive loads when the tool first makes contact with the workpiece and have sufficient compressive and shear strength at elevated temperature to prevent tool fracture or distortion for the duration of the friction stir weld.

1.5.2 Elevated temperature stability:

The tool must maintain strength and dimensional stability during the time of use. Creep (and creep fatigue) is consideration for long weld lengths, where poor creep resistance would change the tool dimensions during welding.

1.5.3 Wear resistance:

Excessive tool wear changes the tool shape, thus changing the weld quality and increasing the probability of defects. In FSW, tool wear can occur by adhesive, abrasive, or chemical wear mechanism. The exact wear mechanism depends on the interaction between workpiece and tool materials and the selected tool parameters.

1.5.4 Tool reactivity:

Tool material must not react with the workpiece or the environment, which would change the surface properties of tool. Titanium is well known to be reactive at elevated temperature, thus any reaction of titanium with the tool material will change the tool properties and alter the joint quality.

1.5.5 Machinability:

Friction stir tools must be designed with features that must be machined, ground or electro discharged machined into the tool.

1.5.6 Uniformity in microstructure and density:

Tool materials are not useful if there are local variations in microstructure or density. These slight variations produce a weak region within the tool where premature facture occurs.

1.6 DESIGN OF TOOL SHOULDER

Tool shoulders are designed to produce heat to the surface and subsurface regions of the workpiece. The tool shoulder produces a majority of the deformational and frictional heating in thin sheet, while the pin produces a majority of the heating in the thick workpiece. Also the shoulder produces the downward forging action necessary for weld.[13,14]

1.6.1 Concave Shoulder

This shoulder is commonly referred as the ***standard-type-shoulder***. Concave tool shoulders produce quality stir welds, and the simple design is easily machined. The shoulder concavity is produced by small angle between the edge of the shoulder and the

pin between 6 and 10^{o}. Concave shoulder design (Fig1.7). Proper operation of this shoulder design requires tilting the tool 2 to 4° from the normal of the work piece away from the direction of travel.

Figure 1.7: Photograph of a concave shoulder with a round bottom pin [13]

1.6.2 Convex Shoulder

Convex shoulders with scrolls move material from the outside of the shoulder in toward the pin. The advantage of the convex shape is that the outer edge of the tool need not to be engaged with the workpiece, so the shoulder can be engaged with the workpiece at any location along the convex surface. Thus a sound weld is produced when any part of the scroll is engaged with the workpiece at any location along the convex surface.

Figure1.8: Photograph of a convex shoulder with a truncated cone pin [13]

1.7 PIN DESIGNS

Friction stirring pins produce deformational and frictional heating to the joint surfaces. The pin is designed to disrupt faying, or contacting surface of the workpiece, shear material in front of the tool, and move the material behind the tool. In addition, the depth of deformation and tool travel speed are governed by the pin design.

1. Round Bottom cylinder pin.(Fig1.7)
2. Truncated cone pin. (Fig1.8)
3. Flat Bottom cylinder pin. (Fig1.9)

Figure 1.9: Photograph of a flat-bottom pin [13]

1.8 WELDING FORCES

During welding a number of forces will act on the tool [8,15]:

1. Downward force:

It maintains the position of the tool at and below the material surface. Some friction-stir welding machines operate under load control but in many cases the vertical position of the tool is preset and so the load will vary during welding.

2. Traverse force:

It acts parallel to the tool motion and is positive in the traverse direction. Since this force arises as a result of the resistance of the material to the motion of the tool it might be expected that this force will decrease as the temperature of the material around the tool is increased.

3. Lateral force:

It acts perpendicular to the tool traverse direction and is defined as positive towards the advancing side of the weld.

4. Torque:

It is required to rotate the tool, the amount of which will depend on the down force and friction coefficient (sliding friction) and/or the flow strength of the material in the surrounding region (sticking friction). The torque decreases with increase in the tool rotation speed due to increase in the heat generation rate and temperature when other variables are kept constant. It becomes easier for the material to flow at high temperatures and strain rates. However, torque is not significantly affected by the change in welding speed .

The torque increases only slightly with the increase in traverse speed because material flow becomes somewhat more difficult at slightly lower temperatures. The torque on the tool can be used to calculate the power required from $P=\omega M$, where M is the total torque on the tool.

1.9 HEAT GENERATION

In FSW, heat is generated by a combination of friction and plastic dissipation during deformation of the metal. Majority of heat generation occurs at the shoulder/workpiece interface. The dominating heat generation mechanism is influenced by the weld parameters, thermal conduct ivies of the work piece, pin tool and weld tool geometry. In the weld, a mixture of recovery and recrystallization phenomena occurs simultaneously. Deformation not only increases the dislocation density but also the amount of grain surface and grain edge per unit volume and by cutting precipitates may force them to dissolve.

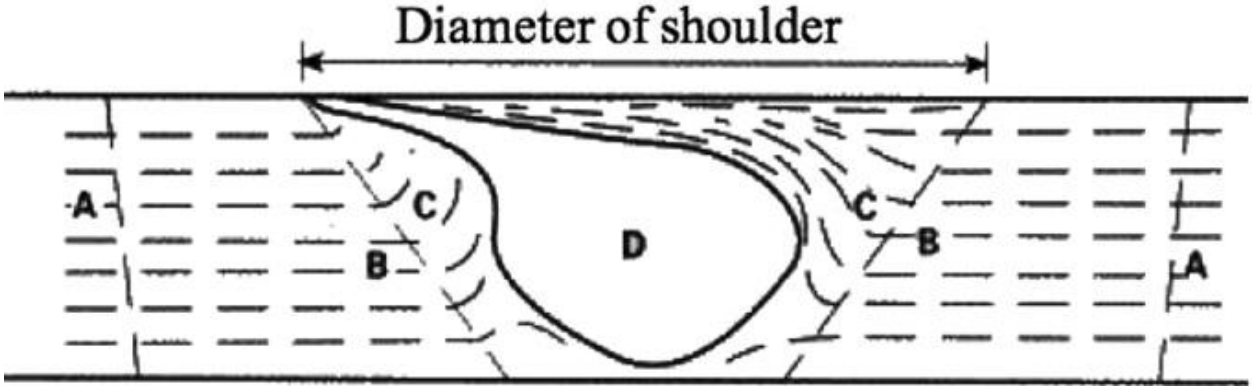

Fig 1.10: Schematic cross-section of a typical FSW weld showing four distinct zones: (A) base metal, (B) heat-affected, (C) thermo-mechanically affected and (D) stirred (nugget) zone [17]

The temperature field around the pin is asymmetric, with slightly higher temperatures reported on the retreating side of the FSW in aluminum alloys. [16,17]

The welding cycle can be split into several stages to determine the heat flow and thermal profile.

- **Dwell period :**
  Where the tool is held stationary relative to the workpiece but still rotating thus the material is preheated by a stationary, rotating tool in order to achieve a sufficient temperature ahead of the tool to allow the traverse. This period may also include the plunge of the tool into the workpiece.

- **Transient heating period:**
  When the tool begins to move there will be a transient period where the heat production and temperature around the tool will alter in a complex manner until an essentially steady-state is reached.

- **Pseudo steady-state**:
  Although fluctuations in heat generation will occur the thermal field around the tool remains effectively constant, at least on the macroscopic scale.

- **Post steady-state:**
  Near the end of the weld heat may 'reflect' from the end of the plate leading to additional heating around the tool.

Heat generation during friction-stir welding arises from two main sources: friction at the surface of the tool and the deformation of the material around the tool. The heat generation is often assumed to occur predominantly under the shoulder, due to its greater surface area, and to be equal to the power required to overcome the contact forces between the tool and the workpiece. The contact condition under the shoulder can be described by **sliding friction**, using a friction coefficient μ and interfacial pressure P, or **sticking friction**, based on the interfacial shear strength ; at an appropriate temperature and strain rate. [18]

1.10 MATERIAL FLOW

Most of the material flow occurs through the retreating side and the transport of the plasticized material behind the tool forms the welded joint.[19] Three types of flow affects the overall transport of plasticized materials during FSW.

- Near the tool, a slug of plasticized material rotates around the tool. This motion is

driven by the rotation of the tool and the resulting friction between the tool and the work-piece.

- Rotational motion of the threaded pin tends to push material downward close to the pin which derives an upward motion of an equivalent amount of material somewhat farther away.
- Relative motion between the tool and the work piece.

1.11. ADVANTAGES OF FRICTION STIR WELDING

Following are some advantages of using friction stir welding process to join any material [8, 20]

- Good mechanical properties (tensile and fatigue) and improves process robustness.
- Improved safety due to the absence of toxic fumes or the spatter of molten material.
- No consumables for e.g. a threaded pin made of conventional tool steel, e.g. hardened H13, can weld over 1000m of aluminium plates and no filler or gas shield is required.
- Easily automated on simple milling machines - lower setup costs and less training.
- Less health and environmental issues.
- Can operate in all positions (horizontal, vertical, etc.), as there is no weld pool.
- Generally good weld appearance thus reducing the need for expensive maching after welding.

1.12 DISADVANTAGES FRICTION STIR WELDING

Following are some disadvantages of friction stir welding that should be kept in mind while performing the process [8]:

- Exit hole left when the tool is withdrawn.
- Large down forces are required with heavy-duty clamping necessary to hold the plates together.
- Less flexible than manual and arc processes (difficulties with thickness variations and non linear welds).
- Often slower traverse rate than some fusion welding techniques.
- It is necessary clamp the workpiece materials firmly. Suitable jigging and backing bars are needed to prevent the abutting plates moving apart.

1.13 APPLICATIONS OF FRICTION STIR WELDING

Friction stir welding is widely being used for joining various materials and in various fields like aerospace, marine, automotive industries and many other commercial applications [8, 21, 22] some of which are described as follows:

1. Shipbuilding and marine industries

The shipbuilding and marine industries are two of the first industry sectors which have adopted the process for commercial applications. The process is suitable for the following applications:

- Panels for decks, sides, bulkheads and floors.
- Aluminum extrusions.
- Hulls and superstructures.
- Helicopter landing platforms.
- Offshore accommodation.
- Marine and transport structures.
- Masts and booms, e.g. for sailing boats

2. Aerospace industry

At present the aerospace industry is welding prototype and production parts by friction stir welding. Opportunities exist to weld skins to spars, ribs, and stringers for use in military and civilian aircraft. The Eclipse 500 aircraft, in which ~60% of the rivets are replaced by friction stir welding, is now in production. Longitudinal butt welds in Al alloy fuel tanks for space vehicles have been friction stir welded and successfully used. The process could also be used to increase the size of commercially available sheets by welding them before forming. The friction stir welding process can therefore be considered for:

- Wings, fuselages, empennages
- Cryogenic fuel tanks for space vehicles.
- Aviation fuel tanks.
- External throw away tanks for military aircraft.
- Military and scientific rockets.
- Repair of faulty MIG welds.
- Various primary and secondary structural components.

3. Railway industry

The commercial production of high speed trains made from aluminum extrusions are joined by friction stir welding. Other applications include:

- High speed trains.
- Rolling stock of railways, underground carriages, trams.
- Railway tankers and goods wagons.
- Container bodies.

4. Land transportation

The friction stir welding process is currently being used commercially, and is also being assessed by several automotive companies and suppliers to this industrial sector for its commercial application. Existing and potential applications include:

- Engine and chassis cradles.
- Wheel rims
- Attachments to hydroformed tubes
- Tailored blanks, e.g. welding of different sheet thicknesses
- . Space frames, e.g. welding extruded tubes to cast nodes
- Motorcycle and bicycle frames.

Friction stir welding is also considered for some other applications for example in refrigeration panels, cooking equipments, gas tanks and cylinders, connecting of aluminium or copper coils used in rolling mills. Following figures shows the parts or elements with have been joined by friction stir welding.

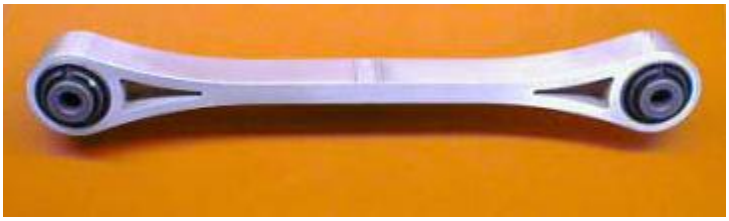

Figure 1.11: Automotive Link Arm Fabricated from Friction Stir Welding [8]

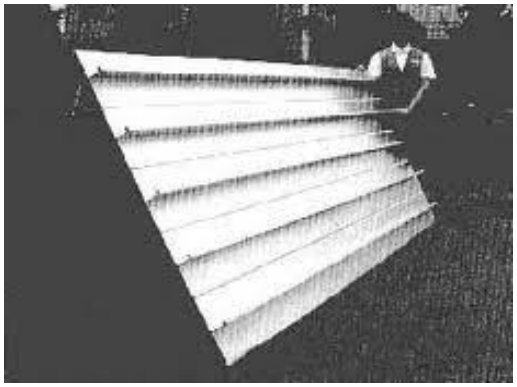

Figure 1.12: Friction Stir Welded Aluminum panels in ship building [8]

Figure 1.13: Japanese railway rolling stock fabricated from aluminum by FSW[20]

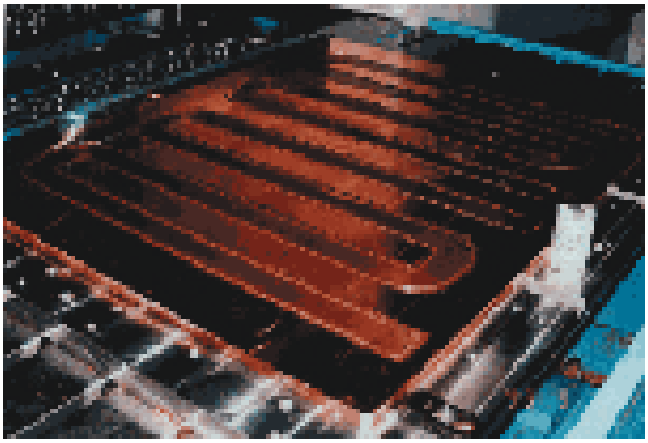

Figure 1.14: Copper backing plate for sputtering used in LCD [8]

CHAPTER 2
LITERRATURE REVIEW

A. Barcellona et al. [23] studied micro structural phenomena occurring in friction stir welding of aluminum alloys. The results of experimental activity on friction stir welding (FSW) of aluminum alloys are reported. Butt joints of two different materials, namely AA2024-T4 and AA7075-T6, were investigated from a metallurgical point of view. Grain dimensions and insoluble particle densities were investigated both in the parent materials and in the joints. The percentage of insoluble particles locally decreases due to the tool pin action. The recrystallization phenomena occurring in the nugget zone contrast the material softening due to precipitates density decrease.

A.K. Hussain and S.A.P. Quadri [24] evaluated the parameters of friction stir welding of AA6351 Aluminum alloy. Experiments were conducted on AA6351 Aluminum alloy in a CNC Vertical Machining Centre. The rotational speed of the tools, the axial pressure and welding speed and the (weld time) are the principal variables that are controlled in order to provide the necessary combination of heat and pressure to form the weld. These parameters were adjusted so that the interface is heated into the plastic temperature range (plastic state) where welding can take place. The Vickers hardness, tensile strength and radiography were considered for investigation by varying tool speed, tool feed and maintaining constant depth of penetration of weld. Results show strong relation and robust comparison between the weldment strength and process parameters. Tensile strength was higher with lower weld speed. This indicates that lower range of weld speed is suitable for achieving maximum tensile strength.

A.P. Reynolds et al. [25] carried out friction stir welding on lap joints to investigate the interface morphology and mechanical properties. Two different materials i.e.iAlcad2024-T3 and Al 7075-T6 that are commonly used in the aerospace industry were joined. Welding variables included welding speed, rotational speed and tool dimensions. A maximum joint efficiency of 86% was achieved for the FSW lap joints. Results indicated that FSW joints, on the basis of strength, potentially replace other joining processes like spot welding and riveting.

G. Çam et al. [26] studied the mechanical properties of friction stir butt-welded Al-5086 H32 plates using different welding speeds at a constant tool rotational speed. The effect

of welding speed on the weld performance of the joints was investigated by conducting optical microscopy, microhardness measurements and mechanical tests (i.e. tensile and bend tests). The effect of heat input during friction stir welding on the microstructure, and thus mechanical properties, of cold-rolled Al- 5086 plates was also determined. The results indicated that the maximum tensile strength of the joints, which is about 75% that of the base plate, was obtained with a traverse speed of 200 mm/min at the tool rotational speed used. On the other hand, the maximum ductility performance of the joints was relatively low. The results showed that both strength and ductility performances can be increased by optimizing the tool penetration depth.

G. Campanile et al. [27] compared the effect of process parameters on mechanical and microstructural properties of AA6056 joints produced by Friction Stir Welding. Different samples obtained by employing rotating speeds of and different welding speeds were produced. The mechanical properties of the joints were evaluated by means of microhardness (HV) and tensile tests at room temperature. Fatigue tests on the welds were carried out by using a resonant electro-mechanical testing machine under constant loading. The microstructure of the materials appeared very fine and equiaxed grains in all the welding conditions.

G.R. Babu et al.[28] studied the effect of processing parameters on mechanical and microstructural properties of aluminum alloy 6082-T6 Friction stir-welded (FSW) joints Different welded specimens were produced by employing variable rotating speeds and welding speeds. Tensile strength of the produced joints was tested at room temperature and the correlation with process parameter was assessed. Microstructures of various zones of FSW welds are presented and analyzed by means of optical microscopy and microhardness measurements. Several studies have been conducted to investigate the properties and microstructural changes in Friction stir welds in the aluminum alloy 6082-T6 in function of varying process parameters. The experimental results indicated that the process parameters have a significant effect on weld macrostructure and mechanical properties of joints.

H. Schmidt et al. [29] worked to establish an analytical model for heat generation by friction stir welding (FSW), based on different assumptions of the contact condition between the rotating tool surface and the weld piece. The material flow and heat generation were characterized by the contact conditions at the interface, and are described as sliding, sticking or partial sliding/ sticking. Experimental results on plunge

force and torque were used to determine the contact condition. The sliding condition yields a proportional relationship between the plunge force and heat generation.

H.J. Liu et al. [30] analyzed the Friction stir welding characteristics of 2017-T351 aluminum alloy sheet. FSW resulted in softening of the 3-mm thick 2017–T351 aluminum alloy sheet, thus the tensile properties of the joints were lower than those of the base material, and the maximum ultimate strength efficiency is 82%. The welding parameters did not significantly affected the tensile properties of the FSW joints, therefore the welding parameters for the 3-mm thick 2017-T351 aluminum alloy sheet can be varied over relatively wide range. All the joints fracture near the weld center and on the Retreating side of the weld. From the viewpoint of inner structures, the fracture locations of the joints occurred at the interface between the weld nugget and the TMAZ on the Retreating side of the weld.

J. Adamowski and M.S. Zkodo [31] investigated the properties and micro structural changes in Friction stir welds in the aluminum alloy 6082-T6 in function of varying process parameters. Tensile strength of the produced joints were tested and the correlation with process parameter was assessed. Microstructures of various zones of FSW welds are presented and analyzed by means of optical microscopy and microhardness measurements. Thus it is found that Mechanical resistance of test welds increases with the increase of travel (welding) speed with constant rotational speed. Softening of the material in weld nugget and heat affected zone was observed, of entity inferior that of fusion welds.

K. Elangovan et al. [32] developed a mathematical model to predict tensile strength of the friction stir welded AA6061 aluminum alloy by incorporating FSW process parameters such as tool rotational speed, welding speed, axial force and tool pin profile using statistical tools such as design of experiments, analysis of variance and regression analysis. Results of this study showed that the joints fabricated using square pin profiled tool with a rotational speed of 1200 rpm, welding speed of 1.25 mm/s and axial force of 7 kN exhibited superior tensile properties compared to other joints.

K. Kimapong and T. Watanabe [33] investigated the effects of pin rotation speed, position of the pin axis, and pin diameter on the tensile strength and microstructure of the butt joint**.** Results showed that the maximum tensile strength of the joint was about 86% of that of the aluminum alloy base metal. Many fragments of the steel were scattered in

the aluminum alloy matrix, and fracture tended to occur along the interface between the fragment and the aluminum matrix. A small amount of intermetallic compounds was formed at the upper part of the steel/aluminum interface, while no intermetallic compounds were observed in the middle and bottom regions of the interface. A small amount of intermetallic compound was also often formed at the interface between the steel fragments and the aluminum matrix. The regions where the intermetallic compounds formed seem to be fracture paths in a joint.

Loureiro et al. [34] investigated the effect of friction stir welding parameters on the microstructure and mechanical properties of welds in two automotive aluminium alloys. Welds were made in 1 mm thick sheets of Al 5182-H111 and Al 6016-T4 alloys. The welding process was carried out in both materials, in two series, using in each series different tool design and welding parameters. The welding parameters were selected in order to give colder welds in the second series than in the first series. Both welding process parameters gave welds with good appearance and free from defects. The central zone of the welds, commonly designated as the nugget, was formed of small equiaxed grains, though these grains are difficult to distinguish in some welds. No substantial changes were observed in the hardness of the welds of the first series as opposed to the welds of the second series in both materials. The change in the process parameters influenced the weld efficiency too.

M.K. Kulekci et al. [35] studied the mechanical properties of welded joints of EN AW-6061-T6 aluminium alloy obtained with friction stir welding (FSW) and conventional metal inert gas welding (MIG) are studied. FSW welds were carried out on a semi-automatic milling machine. The performance of FSW and MIG welded joints were identified using tensile, fatigue, hardness, and impact tests. The joints obtained with FSW and MIG processes were also assessed for distortion that accompanied the welding processes. Taking into consideration the process conditions andrequirements, better tensile, fatigue, and impact strength were obtained with FSW welded joints. The width of the heat affected zone of FSW was narrower than MIG welded joints. The results show that FSW improves the mechanical properties of welded joints.

M.K. Shivaraj and Vijay Dinakaran [36] investigated the micro hardness and mechanical properties of aluminum alloys AA2024–T4 and AA7075–T6 after friction stir welding**.** AA2024–T4 and AA7075–T6. After investigation it was concluded that the welded zone has fine recrystallised grains. Friction stir welding modifies the

microstructure there by eliminating the casting defects present in the cast aluminum alloys. The mechanical properties like micro hardness, yield strength, percentage of elongation and joint efficiencies were superior to the conventional welding methods of aluminum alloys.

N.T. Kumbhar and K. Bhanumurthy [37] carried out trials using a vertical milling machine on Al 6061 alloy. Important process parameters that controlled the quality of the weld that were axial force, rotational speed (rpm), traverse speed (mm/min) and tool tilt angle and these process parameters were optimized to obtain defect free welded joints. It was observed that, during the friction stir welding, extensive deformation is experienced at the nugget zone and the evolved microstructure strongly affects the mechanical properties of the joint. The optimization of process parameters and also highlighted the influence of post weld heat treatment PWHT on the microstructure, composition variation across the interface and mechanical properties of FSW 6061 Al alloy.

P. Cavaliere at al. [38] analyzed the mechanical and microstructural properties of 2024 and 7075 aluminum alloys joined together by friction stir welding. These two materials were welded and after were tested in tension at room temperature in order to analyze the mechanical response and to observe the differences with the parent materials, the tensile response of the material in longitudinal direction revealed an increase in strength respect to the transverse one. The microstructure resulting from the FSW process was studied by employing optical and scanning electron microscopy.

T.J. Lienert et al. [39] worked on the feasibility of friction stir welding (FSW) for joining of mild steel. Defect-free welds were produced on 0.25-in. plates. Comparisons before and after welding combining both metallographic and metrology techniques suggest changes in tool dimensions stem from both rubbing wear and deformation of the tool. The greatest changes in tool dimensions occurred during the initial plunging stage. Microstructures of the welds were examined using optical and scanning electron microscopy. The weld region displayed several microstructurally distinct regions. Peak surface temperatures close to 1000°C (1832°F) were measured on the tool above the shoulder during FSW using thermocouples and an infrared camera system.

T. Sakthivel and J. Mukhopadhyay [40] applied friction stir welding technique to joining 2 mm thick copper sheet. Mechanical and microstructural analysis has been

performed to evaluate the characteristics of friction stir welded copper. The microstructure of the weld nugget (WN) consists of fine equiaxed grains. Similarly, the elongated grains in the thermomechanically affected zone (TMAZ) and coarse grains in the heat-affected zone (HAZ) were observed. The hardness values in the Weld Nugget were higher than the base material. Eventually HAZ shows lowest hardness values because of few coarse grains presence. Friction stir welded copper joints passes 85% weld efficiency as compared to the parent metal.

Yan Qiu and Wen Zhang [41] worked on dissimilar friction stir welding between 5052 Al alloy and AZ31 Mg alloy with the plate thickness of 6 mm was investigated. Sound weld were obtained at rotation speed of 600 r/min and welding speed of 40 mm/min. Compared with the base materials, the microstructure of the stir zone is greatly refined. Complex flow pattern characterized by intercalation lamellae is formed in the stir zone. Microhardness measurement of the dissimilar welds presents an uneven distribution due to the complicated microstructure of the weld, and the maximum value of microhardness in the stir zone is twice higher than that of the base materials. The tensile fracture position locates at the advancing side (aluminum side), where the hardness distribution of weld shows a sharp decrease from the stir zone to 5052 base material.

W. David Kelton [42] introduced some of the ideas, issues, challenges, solutions, and opportunities in deciding how to experiment with a simulation model to learn about its behavior. Careful planning, or designing, of simulation experiments is generally a great help, saving time and effort by providing efficient ways to estimate the effects of changes in the model's inputs on its outputs. Traditional experimental-design methods were introduced in the context of simulation experiments, as are the broader questions pertaining to planning computer-simulation experiments.

CHAPTER 3
PROBLEM FORMULATION

3.1 PROPOSED WORK

From the review of the available literature it is evident that the aluminum alloys are being used effectively for many applications such as automotive, aerospace, shipbuilding etc because of their high mechanical strength to weight ratio.

Most of the current welding procedure for welding aluminum alloys are to be operated under inert conditions and are costly and require use of filler material, which further creates problem of mismatch in mechanical properties of weld and base metal.

Whereas friction stir welding provides a solid state approach for joining the materials without use of any external filler material. This approach is useful for welding aluminum alloys and other materials and their alloys which are difficult to join by any other methods.

From the available literature it is seen that not much work have been done on welding of Aluminum AA6063 and of 12 mm thickness.

In the present thesis work it is proposed to apply friction stir welding technique to 12 mm thick AA 6063 sheets on vertical milling machine. Important process parameters that controlled the quality of the weld that are rotational speed (rpm), traverse speed (mm/min), tool tilt angle, tool plunge depth (mm) are optimized to obtain defect free welded joint. Tool of specific dimensions is to be prepared on lathe machine to obtain sound weld.

Subsequently, efforts were made to find out the mechanical properties like hardness, tensile strength, percentage elongation and microstructual analysis to evaluate the characteristics of friction stir welded aluminium.

3.1.1 OBJECTIVES

1. To study the mechanical properties –Tensile strength, hardness number and impact energy of friction stir welded joints with respect to parent material.
2. Maximum temperature of the welded zone.
3. To visualize presence of any joint remnants.

Following are the tests that are to be performed on the welded plates.

1. The Microstructure.
2. Ultimate Tensile Test.
3. Impact Test.
4. Rockwell Hardness Test.

3.2 WORK PLAN

Following is the flow chart of above discussed objectives and method.

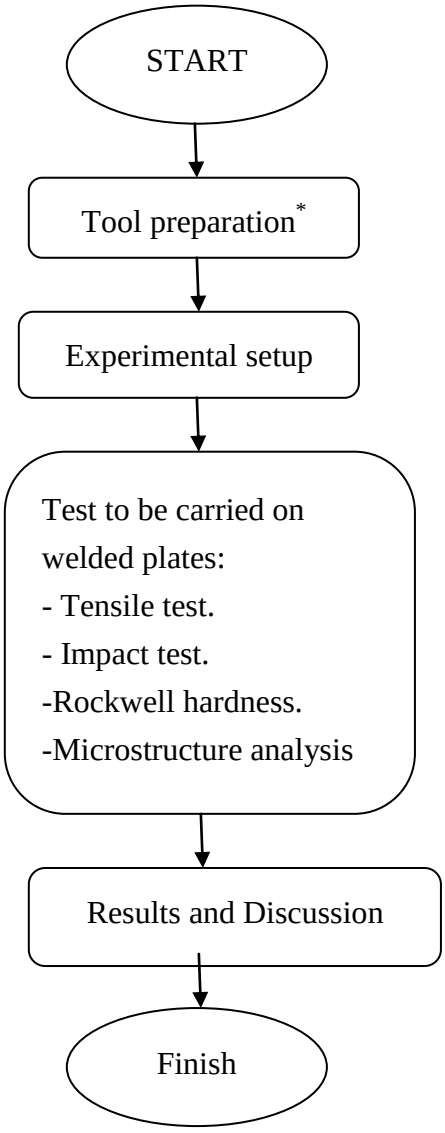

Figure 3.1: Flow chart for work plan

***Tool preparation**

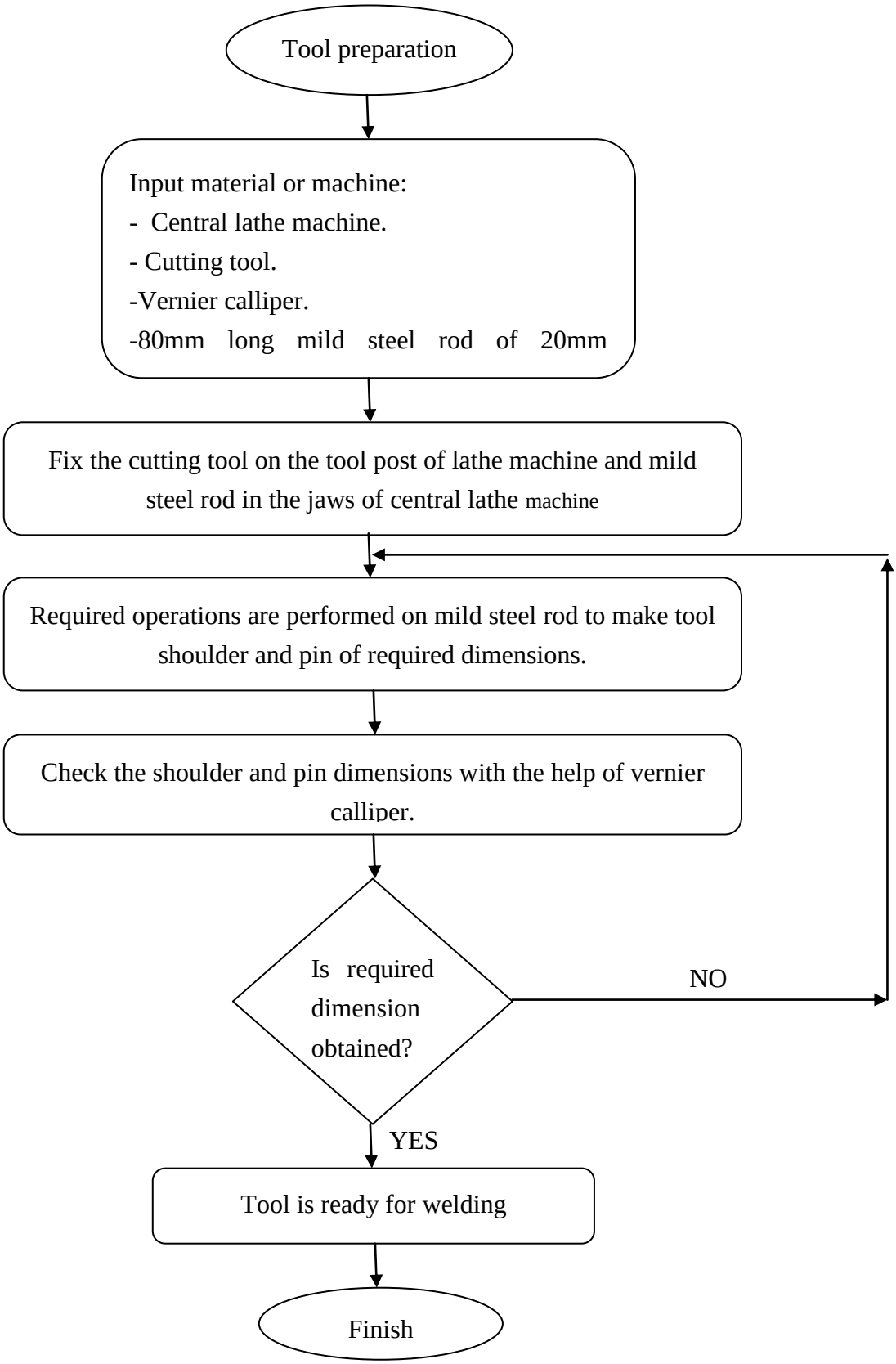

Figure 3.2: Flow chart of tool preparation

CHAPTER 4

METHODOLOGY

4.1 THEORITICAL METHODOLOGY

An analytical model for heat generation by friction stir welding [25,29], based on different assumptions of the contact conditions between the rotating tool surface and the weld piece is established. The material flow and heat generation are characterized by the contact conditions at the interface, and are described as sliding, sticking or partial sliding/sticking.

A schematic representation of the set-up is illustrated in figure4.1.Figure 4.2.shows a simplified tool design. In this process, two tool surfaces are needed to perform the heating and joining processes in the friction stir weld. The shoulder surface is the area where the majority of the heat is generated, whereas the probe surface is where the work pieces are joined together and only a fraction of the total heat is generated. Second, the shoulder confines the underlying material so void formation and porosity behind the probe are prevented. The conical tool shoulder helps establish a pressure under the shoulder, but also acts as an escape volume for the material displaced by the probe during the plunge action (figure 4.1).

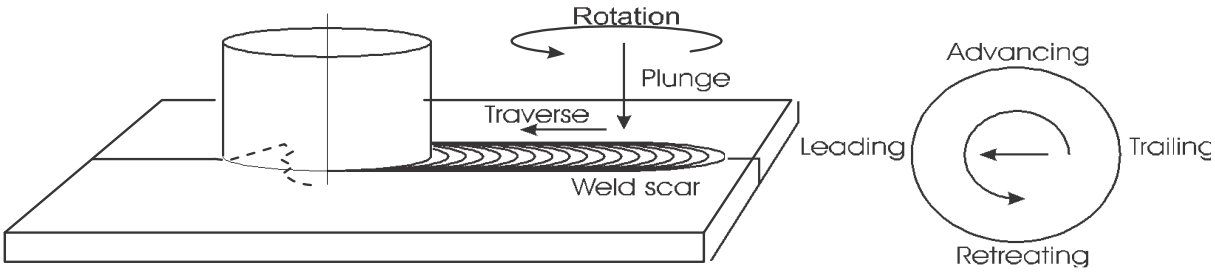

Figure 4.1: Schematic of the weld set up and definition of orientations [29]

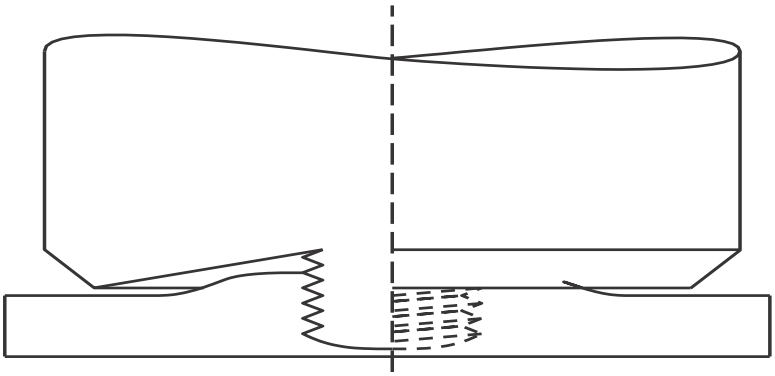

Figure4.2: Side view of the FSW tool showing the conical shoulder cap and threaded probe. [29]

4.1.1 Contact Condition

When modeling the FSW process, the contact condition is the most critical part of the numerical model. In this case, the Coulomb law of friction is applied to describe the shear forces between the tool surface and the matrix. In general, the law estimates the contact shear stress as

$$\tau_{contact} = \mu p = \mu \sigma \tag{4.1}$$

Where μ is the friction coefficient, p and σ are the contact pressures. Coulomb's law predicts the mutual motion between the two segments-whether they stick or slide. The top surface segment originates from the tool and moves with a velocity of ωr, where ω is the rotational speed and r is the distance from the surface segment to the rotation axis. The lower surface segment originates from the matrix. The normal interpretation of Coulomb's law is based on rigid contact pairs, without considering internal stress. For this, the three following contact states are defined.

- **Sticking condition**

  The matrix surface will stick to the moving tool surface segment, if the friction shear stress exceeds the yield shear stress of the underlying matrix. In this case, the matrix segment will accelerate along the tool surface (finally receiving the tool velocity), until equilibrium state is established between the contact shear stress and the internal matrix shear stress. At this point, the stationary full sticking condition is fulfilled.

- **Sliding condition**

  If the contact shear stress is smaller than the internal matrix yield shear stress, the matrix segment volume shears slightly to a stationary elastic deformation, where the shear stress equals the 'dynamic' contact shear stress. This state is referred to as the sliding condition.

- **Partial sliding/sticking**

  This is the mixed state between two sticking and sliding condition. In this case, the matrix segment accelerates to a velocity less than the tool surface velocity, where it stabilizes. The equilibrium establishes when the 'dynamic' contact shear stress equals the internal yield shear stress due to a quasi-stationary plastic deformation rate. This is referred to as the partial sliding/sticking condition.

Table 4.1 summarizes the relationship between the different contact conditions. δ is a contact state variable, which relates the velocity of thecontact points at the matrix surface relative to the tool point in contact.

Condition	Tool velocity	Shear stress	State variable
Sticking	$V_{tool} = \omega r$	$\tau_{friction} > \tau_{contact}$	$\delta = 1$
Sticking/sliding	$V_{tool} = \omega r$	$\tau_{friction} \geq \tau_{yield}$	$0 < \delta < 1$
Sliding	$V_{tool} = \omega r$	$\tau_{friction} < \tau_{yield}$	$\delta = 0$

Table 4.1 Definition of contact condition, velocity/shear relationship and state variable

4.1.2 Analytical Estimation of Heat Generation

Three different analytical estimations are made, all of which are based on a general assumption of uniform contact shear stress $\tau_{contact}$ and further distinguished by assuming a specific contact condition. In the first estimation, a sticking interface condition *(δ = 1)* is assumed and in the second estimation a pure sliding *(δ = 0)* interface described by a Coulomb friction condition is assumed. In the case of the sticking condition, the shearing is assumed to occur in a layer very close to the interface and in the sliding condition the shear is assumed to take place at the contact interface. The third estimation is used in the case where the partial sliding/sticking condition is assumed.

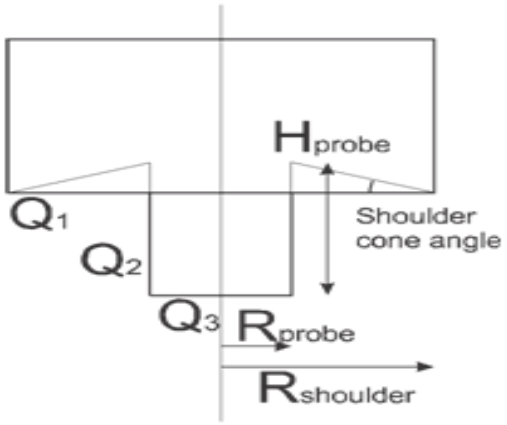

Figure4.3: Heat generation contributions in analytical estimates [11]

During the FSW process, heat is generated at or close to the contact surfaces, which have complex geometries according to the tool geometry (figure 4.3), but for the analytical estimation, a simplified tool design with a conical shoulder surface, a vertical cylindrical probe side surface and a horizontal (flat) probe tip surface is assumed. The conical shoulder surface is characterized by the cone angle α, which in the case of a flat shoulder, is zero. The simplified tool design is presented in figure4.3, where $\mathbf{Q_1}$ is the heat generated under the tool shoulder, $\mathbf{Q_2}$ at the tool probe side and $\mathbf{Q_3}$ at the tool probe tip, hence the total heat generation, $\mathbf{Q_{Total}} = Q_1 + Q_2 + Q_3$. Following are the equations of the heat generated by all the parts of tool.

1. Heat generation from the shoulder:

The shoulder surface of a modern FSW tool is in most cases concave or conically shaped. The purpose of this geometric feature is to act as an escape volume as the probe is submerged into the matrix during the plunge operation, secondarily enhancing the extrusion and consolidation of the material during the weld operation.

$$Q_1 = {}^{2}/_{3}\,\pi_{contact}\,\omega\,(R^3_{shoulder} - R^3_{probe})(1 + tan\alpha) \qquad (4.2)$$

2. Heat generation from the probe.

The probe is simplified to a cylindrical surface with a radius of *R*probe and a probe height *H*probe. The heat generated from the probe consists of two contributions; *Q*2 from the side surface and *Q*3 from the tip surface.

$$Q_2 = 2\pi\tau_{contact}\omega R_{probe}^2 H_{probe} \quad (4.2)$$

$$Q_3 = {}^{2}/_{3}\,\pi\tau_{contact}\,\omega R_{probe}^3 \quad (4.3)$$

The three contributions are combined to get the total heat generation estimate Q_{total}

$$Q_{total} = Q_1 + Q_2 + Q_3 \quad (4.4)$$

3. Shear stress for sticking condition

If the sticking interface condition is assumed, the matrix closest to the tool surface sticks to it. The layer between the stationary material points and the material moving with the tool has to accommodate the velocity difference by shearing. The yield shear stress τ_{yield} is estimated to be $\sigma_{yield}/\sqrt{3}$, where σ_{yield} is the weld material yield stress. This result is readily obtained by comparing von Mises yield criterion in uniaxial tension andpure shear. The contact shear stress is then

$$\tau_{yield} = {}^{\sigma_{yield}}/_{\sqrt{3}} \quad (4.5)$$

The yield stress is independent of pressure, but highly temperature dependent. If the same shear yield stress is applied all over the interface, the assumption of an isothermal interface follows. This gives a modified expression of (4.4), assuming the sticking condition

$$Q_{total,sticking} = {}^{2}/_{3}\,\pi\,{}^{\sigma_{yield}}/_{\sqrt{3}}\,\omega((R_{shoulder}^3 - R_{probe}^3)(1 + tan\alpha) + R_{probe}^3 + 3R_{probe}^2 H_{probe} \quad (4.6)$$

4. Shear stress for sliding condition.

Assuming friction interface conditions where the tool surface and weld material are sliding against each other, the frictional shear stress $\tau_{friction}$ is introduced in the general equation (4.4). Coulomb's friction law describes the shear stress the critical friction stress necessary for a sliding condition as

$$\tau_{contact} = \tau_{friction} = \mu p = \mu\sigma \quad (4.7)$$

where μ is the friction coefficient, and p and σ are the contact pressures. Thus, for the sliding condition, the total heat generation is given by

$$Q_{total,sliding} = {}^{2}/_{3}\,\pi\mu p\,\omega\left(\left(R_{shoulder}^{3} - R_{probe}^{3}\right)(1+tan\alpha) + R_{probe}^{3} + 3R_{probe}^{2}H_{probe}\right) \tag{4.8}$$

5. Heat generation ratios

Based on the geometry of the tool and independent of the contact condition, the ratio of heat generation, i.e. contributions from the different surfaces compared to the total heat generation, are as follows:

$$\textbf{a) } f_{shoulder} = \frac{Q_1}{Q_{total}} = \frac{\left(R_{shoulder}^{3} - R_{probe}^{3}\right)(1+tan\alpha)}{\left(R_{shoulder}^{3} - R_{probe}^{3}\right)(1+tan\alpha)+R_{probe}^{3}+3R_{probe}^{2}H_{probe}} \tag{4.9}$$

$$\textbf{b) } f_{probe\ side} = \frac{Q_2}{Q_{total}} = \frac{3R_{probe}^{2}H_{probe}}{\left(R_{shoulder}^{3} - R_{probe}^{3}\right)(1+tan\alpha)+R_{probe}^{3}+3R_{probe}^{2}H_{probe}} \tag{4.10}$$

$$\textbf{c) } f_{probe\ tip} = \frac{Q_3}{Q_{total}} = \frac{R_{probe}^{3}}{\left(R_{shoulder}^{3} - R_{probe}^{3}\right)(1+tan\alpha)+R_{probe}^{3}+3R_{probe}^{2}H_{probe}} \tag{4.11}$$

4.2 EXPERIMENTAL METHODOLOGY

4.2.1 Experimental Setup for Friction Stir Welding

For preparing Friction stir welding plates and testing of weld samples following machines/equipments were used:

- Lathe machine.
- Vertical milling machine.
- Shaper machine.
- Laser thermocouple.
- Power hacksaw.
- Band saw.
- Belt grinder.

- Optical microscope.

4.2.2 Details of materials used

A brief description of material used in friction stir welding process is given below:

1. Mild Steel:

Mild steel has high tensile and impact strength. Mild steel is especially desirable for construction due to its weldablility and machinability. Because of its high strength and malleability it is quite soft.

Thus the tool was made from mild steel by cutting it from the available rods of 200mm diameter.

Chemical composition of mild steel is given in table4.2

Element	C	Si	Mn	S	P	Ni	Cr
Wt%	0.44	0.4	1.65	0.01	0.017	0.09	0.152

Table 4.2 Composition of Mild Steel

2. Aluminium Alloy 6063

AA 6063 is an aluminium alloy, with magnesium and silicon as the alloying element. It has good mechanical properties and is heat treatable and weldable. AA6063 is mostly used in extruded shapes for architecture, particularly for window frames , door frames and roofs.

Chemical composition of AA6063 is given in table4.3

Element	Si	Fe	Cu	Mn	Mg	Cr	Zn	Ti	Al
Wt%	0.42	0.35	0.1	0.1	0.74	0.1	0.1	0.1	98.9

Table 4.3 Composition of 6063 aluminium alloy

4.2.3 Tool Preparation

The friction stirring tool consists of pin or probe and shoulder. The pin length is determined by the workpiece thickness. It should be slightly smaller than the workpiece thickenss. Pin diameter should be small enough to allow consolidation of the workpiece material behind the tool before the material cools. Tool shoulders are designed to produce heat in the surface and subsurface regions of the workpiece. It restricts the metal flow to a level equivalent to the shoulder position i.e. approximately to the initial workpiece top surface.

The tool type used in this experiment is round bottom cylindrical pin with concave

shoulder (Fig4.5) prepared on the lathe machine by performing facing, turning, tapering and threading operations (Fig4.4)

Tool Dimensions:

Length of tool:	70 mm
Radius of tool shoulder:	9 mm
Height of tool shoulder:	15mm
Radius of tool pin:	3 mm
Height of tool pin:	10 mm

Figure 4.4: Tool prepared on lathe machine

Figure 4.5 Tool fixed on milling m/c

4.2.4 Welding Parameters

The AA 6063 plates were welded using two different tool rotational speed, tool traverse speed, tool tilt and plunge depth. The tool rotation speeds used in this experiment were 1120 rpm and 1800 rpm. The tool traverse speeds of 16 mm/min and 31.5 mm/min were used. Tool tilt was maintained 1^o and 2^o during the experiment. Plunge depth was varied from 6 mm to 10mm. Some parameters were varied while the plates dimensions were kept constant throughout the experiment.

1. Varying parameters

Following were the four parameters which were varied during the experiment:

- **Tool rotational speed (rpm)**: Tool Rotational Speed means how fast the tool rotates.
- **Tool tilt angle:** Tool tilt is given by tilting the tool by 2-4 degrees, such that the rear of the tool is lower than the front.
- **Plunge depth (mm):** The plunge depth is defined as the depth of the lowest point of the shoulder below the surface of the welded plate.

- **Traverse speed (mm/min):** Traverse Speed means how quickly the tool travels the interface of the specimen.

2. Fixed parameters

The following were the three parameters which were kept constant throughout the experiment:

- Length of plates.
- Width of plates
- Thickness of plates.

4.2.5 TEST MATRIX

For parameters Tool Rotational Speed, Tool tilt, Traverse Speed, Plunge depth were varied at two levels:

S.No	Process Parameters	Notations	Units	Levels	
1.	Tool rotational speed	A	rpm	- (Low)	+ (High)
2.	Tool tilt	B	Degree	- (Low)	+ (High)
3.	Plunge depth	C	mm	- (Low)	+ (High)
4.	Traverse speed	D	mm/min	- (Low)	+ (High)

Table 4.4: Test matrix

Nunber of levels=2

Nunber of factors (K) =4

Formula used= $(\text{Level})^{\text{Factor}} = 2^K = 2^4 = 16$

Total number of experiments is 16. Therefore sixteen plates at various conditions are to be welded.

Table 4.3 shows the design matrix that is to be applied for performing the experiments.

Experiment Number	Factors			
	A	B	C	D
1.	-	-	-	-
2.	+	-	-	-
3.	-	+	-	-
4.	+	+	-	-
5.	-	-	+	-
6.	+	-	+	-
7.	-	+	+	-
8.	+	+	+	-
9.	-	-	-	+
10.	+	-	-	+
11.	-	+	-	+
12.	+	+	-	+
13.	-	-	+	+
14.	+	-	+	+
15.	-	+	+	+
16.	+	+	+	+

Table 4.5: Design matrix for a 2^4 factorial experimental

By substituting the low and high level values of different parameters in above table it is transformed as shown in table 4.4:

Experiment Number	Factors			
	A	B	C	D
1.	1120	1	6	16
2.	1800	1	6	16
3.	1120	2	6	16
4.	1800	2	6	16
5.	1120	1	10	16
6.	1800	1	10	16
7.	1120	2	10	16
8.	1800	2	10	16
9.	1120	1	6	31.5
10.	1800	1	6	31.5
11.	1120	2	6	31.5
12.	1800	2	6	31.5
13.	1120	1	10	31.5
14.	1800	1	10	31.5
15.	1120	2	10	31.5
16.	1800	2	10	31.5

Table 4.6: Test matrix showing parameters varied at different levels and number of experiments.

4.2.6 EXPERIMENTAL PROCEDURE

Following procedure was followed after tool was prepared of required dimension:

1. Two AA 6063 plates with dimensions 270 mmx 10mm x12 mm (L x b x t) respectively were placed on a backing plate in a manner that prevents the abutting joint faces from being apart and clamped firmly on the vice of vertical milling machine.

2. Tool was fixed firmly in the tool collect of respective dimension and rotated at required rpm.

3. Tool pin is plunged vertically into the joint line between the workpieces, while the tool is rotating. Due to velocity difference between the rotating tool and the stationary work piece, heat is produced by frictional work and material deformation is started.

4. To accomplish the welding, the rotating tool is traversed along the line, while the shoulder of the tool is maintained in intimate contact with the plate surface. Shoulder confirms the underlying material so void formation and porosity behind the probe are prevented.

5. Temperature is measured during the complete process at the midpoint of plates with the help of laser thermocouple.

6. As the heat dissipated into the surrounding material, the temperature rises and material softens without reaching the melting point (hence known as solid state process).

7. As the pin is moved in the direction of the welding leading face of pin, assisted by a specified pin profile, forces plasticized material to the back of the pin whilst applying a substantial forging force to consolidate the weld metal.

8. When the weld distance is covered, the tool is pulled out of the workpiece leaving behind an exit hole as a foot print of the tool.

A schematic representation of the experimental setup in four steps is illustrated in fig 4.6

Figure 4.6: Plates are clamped firmly and tool is fixed.

Figure 4.7 Rotating tool is inserted between the joining line of plates up to desired plunge depth

Figure 4.8 Tool is subsequently traversed along the joining line

Figure 4.9: Measurement of temperature at mid point with the help of laser thermocouple.

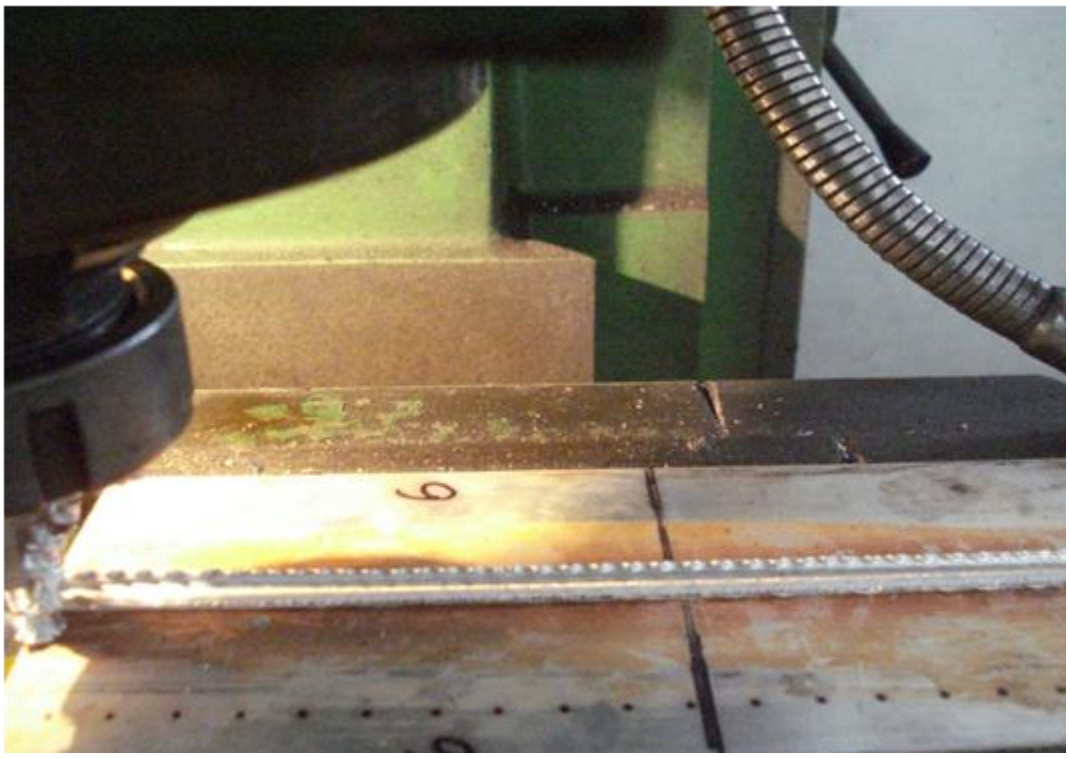

Figure 4.10: **Tool is pulled out when the joining is complete leaving the exit hole behind**

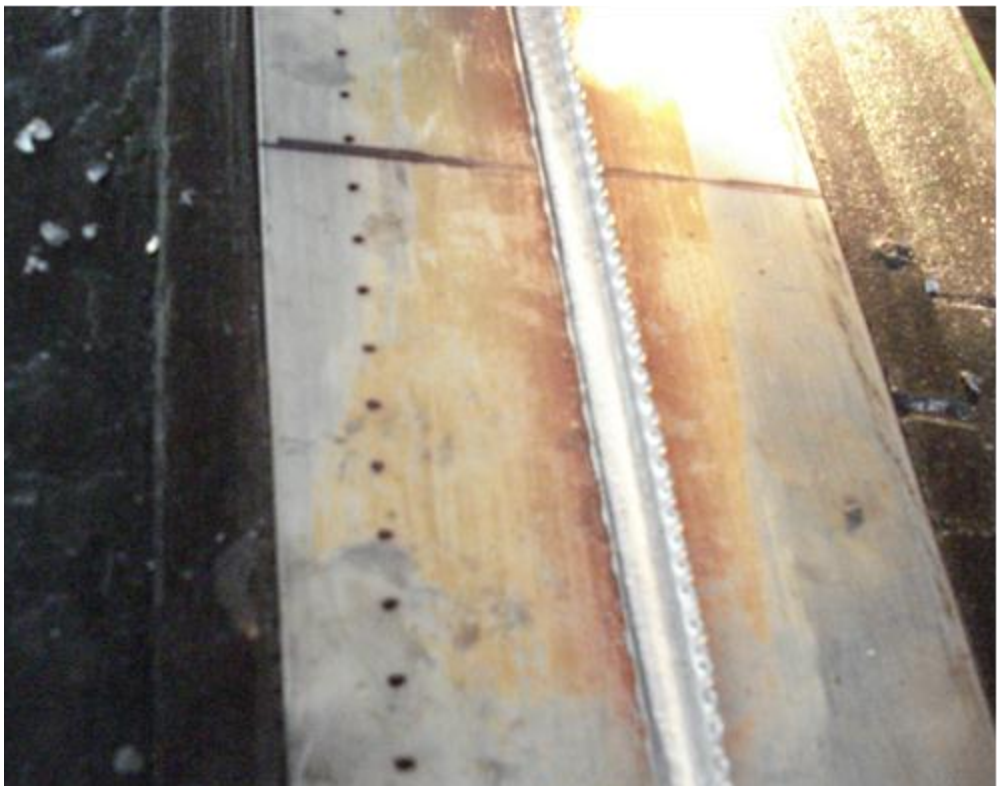

Figure 4.11: Friction stir welded plate.

4.3 TESTING PERFORMED

4.3.1 Tensile Test:

Ultimate tensile strength (UTS), or tensile strength (TS) or ultimate strength, is the maximum stress that a material can withstand while being stretched or pulled before necking. Tensile strength is defined as a stress, which is measured as force per unit area.

This test was performed on universal testing machine (Fig 4.14). Specimen for this testing having dimensions 220mmx60mmx60mm (Fig 4.13) were cut from the welded plate on power hacksaw (Fig4.12) and prepared on vertical milling machine. An extensometer was fixed on the specimen to obtain load v/s extension graph.

Figure 4.12: Sample preparation on power hacksaw

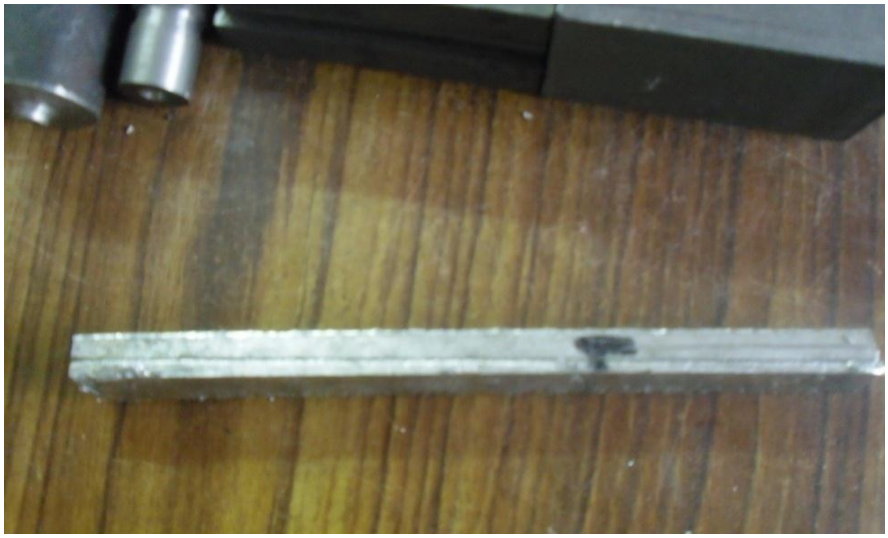

Figure4.13: Specimen for tensile testing.

Figure4.14: Testing on Universal Testing machine with extensometer attached

4.3.2 Rockwell Hardness Test

The Rockwell test determines the hardness by measuring the depth of penetration of an indenter under a large load compared to the penetration made by preload. There are different Rockwell scales, which are denoted by a single letter, that use different loads or indenters.

The scale used in this experiment is *B Scale* that uses load100 kgf and has $^{1}\!/_{16}$-inch-diameter (1.588 mm) steel sphere indenter and is mainly used for testing Aluminium,

brass, and soft steels. Thus the hardness obtained is called HRB.

Samples of dimensions 100mmx10mmx10mm were prepared on band saw (Fig4.15) and vertical milling machine and tested on Rockwell hardness testing machine.(Fig4.16)

Figure 4.15 Samples preparation on band saw

Figure 4.16: Rockwell hardness testing machine

Rockwell hardness number was noted at 10 points on each specimen. Firstly it was tested at weld centre i.e. on the weld line. After that hardness was tested at 10 mm distance on both the sides from the centre line i.e known as stir zone. In this zone hardness at three points were checked for accuracy. Second, at 20 mm distance on both the sides from the weld centre i.e. heat-affected zone. Third at 30 mm distance on both the sides from the weld centre i.e. the parent material.

4.3.3 Izod Impact Test

A notched sample is used to determine the impact strength. An arm held at a specific height (constant potential energy) is released. The arm hits the samples and breaks it. From the energy absorbed by the sample, its impact strength is determined.

Samples of dimensions 75mmx10mmx10mm for this test were prepared on band saw and vertical milling machine. V-notch at a distance of 28mm and 45° angle is given on each sample on shaper machine (Fig 4.15)

Figure 4.17 Samples prepared on Shaper machine

Figure 4.18 Izod impact testing machine

4.3.4 Optical Microscopy

The cross section of weld samples were examined under the optical microscope to determine the structure. Pieces from each welded plate of dimension 10mmx10mmx10mm were cut on band saw. The pieces were polished using 100, 150, 220, 400, 600 grit silicon carbide paper (Fig 4.17). They were than etched with keller etchent and examined through Lieca optical microscope (Fig 4.22).

Figure4.19: Belt Grinder used for polishing of samples

Figure 4.20: Samples before polishing

Figure 4.21: Samples after polishing

Figure 4.22: Lieca optical microscope

Each sample was seen two magnifications for better interpretation of results. First at 10x magnification and second at 20x magnification under Lieca optical microscope.

CHAPTER 5
RESULTS AND DISCUSSIONS

5.1 ANALYTICAL ESTIMATION OF HEAT GENERATION

The tool dimensions for this calculation are:

Tool shoulder radius, m	= $R_{shoulder}$	= 9mm	= 0.009m
Tool probe radius, m	= R_{probe}	= 3mm	=0.003m
Tool probe height, m	= H_{probe}	= 10mm	= 0.01m
Tool shoulder cone angle	= α	= 8.5°	
Friction coefficient, μ	0.6	for static condition	
Friction coefficient, μ	0.4	for sliding condition	
Contact shear stress, $\tau_{contact}$	= 69 MPa	= 69 x 10^6 Pa	
Friction shear stress, $\tau_{friction}$	= μp		
Yield stress, σ_{yield}	= 48 MPa	= 48 x 10^6 Pa	
Tool angular rotational speed, rad/s	$=\omega_1 = 2\pi N/60$ = 117.286 rad/s	(N_1 = 1120 rpm)	
	$=\omega_2 = 2\pi N/60$ = 188.495 rad/s	(N_2 = 1800 rpm)	

On substituting known values of the parameters, tool dimension, and all other values in derived equations (chapter 4), the heat generation values are as follows:

i) Heat Generation from the shoulder: from equation 4.2 the values are-

a) For tool angular rotational speed ω_1 = 117.286 rad/s

Q_1 = 13683.23W

b) For tool angular rotational speed ω_2 = 188.495 rad/s

Q_1 = 20843.52W

ii) Heat Generation from the shoulder: from equation 4.3 and 4.4 the values are-

a) For tool angular rotational speed ω_1 = 117.286 rad/s

Q_2 = 4576.33 W

Q_3 = 457.63 W

b) For tool angular rotational speed ω_2 = 188.495 rad/s

Q_2 = 7354.80W

Q_3 = 735.48 W

iii) Total heat generated: from equation 4.4 the values are-

a) For tool angular rotational speed ω_1 = 117.286 rad/s

Q_{total} = 18717.19 W

b) For tool angular rotational speed ω_2 = 188.495 rad/s

Q_{total} = 28933.8 W

iv) For sticking condition heat generated: from equation 4.6 the values are

a) For tool angular rotational speed ω_1 = 117.286 rad/s

$Q_{total,\ sticking}$ = 7487.45W

b) For tool angular rotational speed ω_2 = 188.495 rad/s

$Q_{total,\ sticking}$ = 12033.38W

v) For sliding condition heat generated: from equation 4.7 the values are

a) For tool angular rotational speed ω_1 = 117.286 rad/s

$Q_{total,sliding}$ = 18644.32W

b) For tool angular rotational speed ω_2 = 188.495 rad/s

$Q_{total,sliding}$ = 29964.03W

5.1.2 Heat Generation ratios:

Based on the heat generated from independent contact conditions, contributions from different surfaces compared to the total heat generated are as follows

i) $f_{shoulder}$ = 0.73

ii) $f_{probe\ side}$ = 0.24

iii) $f_{probe\ tip}$ = 0.0244

This indicates that, for the specific tool geometry, the tool shoulder contributes major fraction of heat generation whereas the probe tip heat generation is negligible as compared to that of total heat generated.

5.2 TEMPERATURE PROFILE

Following table shows the temperature profile and peak temperatures for all the specimens. The temperature was recorded at single point during complete process which took around 10 minutes for each plate.

Number of Experiments	Parameters				Peak Temperature
Sample Number	Tool RPM	Tool Tilt	Plunge D	Traverse Speed	(Degree celsius)
1	1120	1	6	16	185.4
2	1800	1	6	16	192.6
3	1120	2	6	16	200.1
4	1800	2	6	16	168.3
5	1120	1	10	16	169.5
6	1800	1	10	16	180.8
7	1120	2	10	16	218.4
8	1800	2	10	16	250.2
9	1120	1	6	31.5	195.8
10	1800	1	6	31.5	192.6
11	1120	2	6	31.5	162.2
12	1800	2	6	31.5	242.4
13	1120	1	10	31.5	180.3
14	1800	1	10	31.5	218.4
15	1120	2	10	31.5	185.6
16	1800	2	10	31.5	251.4

Table 5.1: Test matrix for peak temperature

Following are the plots of temperature vs time for welds made different welding speeds.

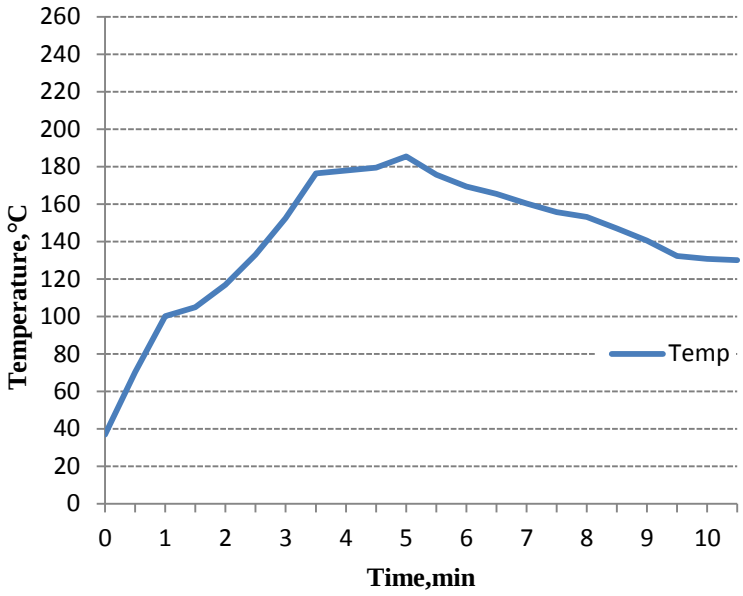

Figure 5.1: Temperature vs. Time graph for specimen no 1

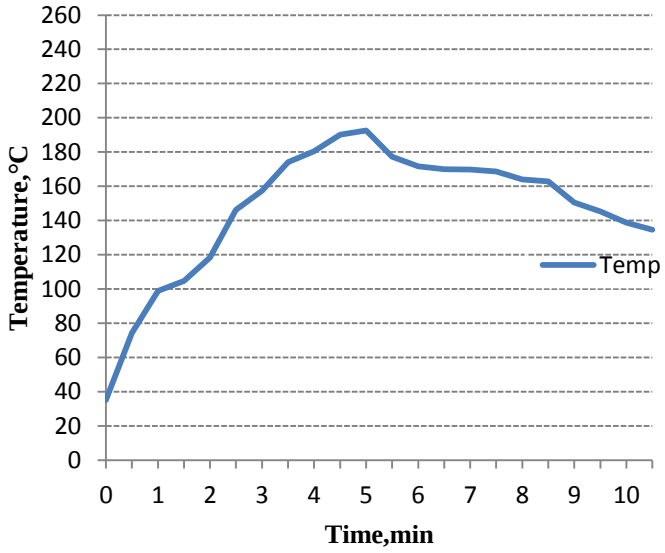

Figure 5.2: Temperature vs. time graph for specimen no 2

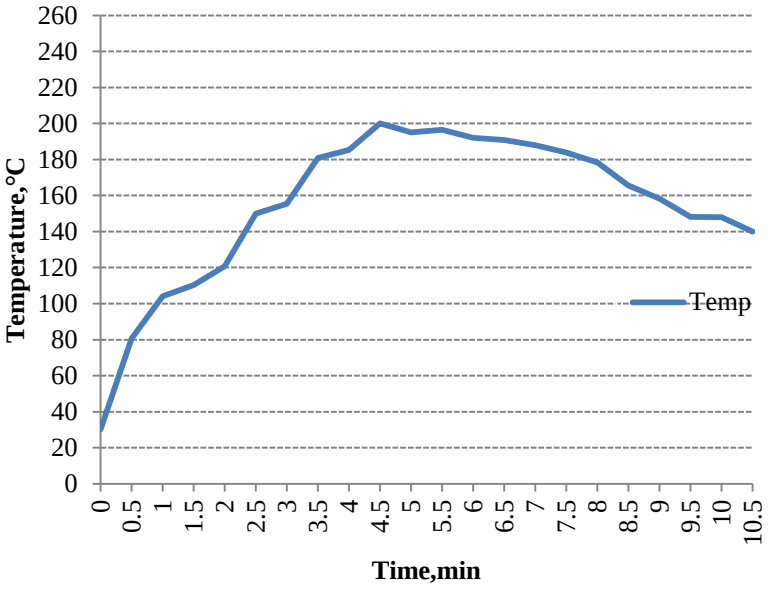

Figure 5.3: Temperature vs. time graph for specimen no 3

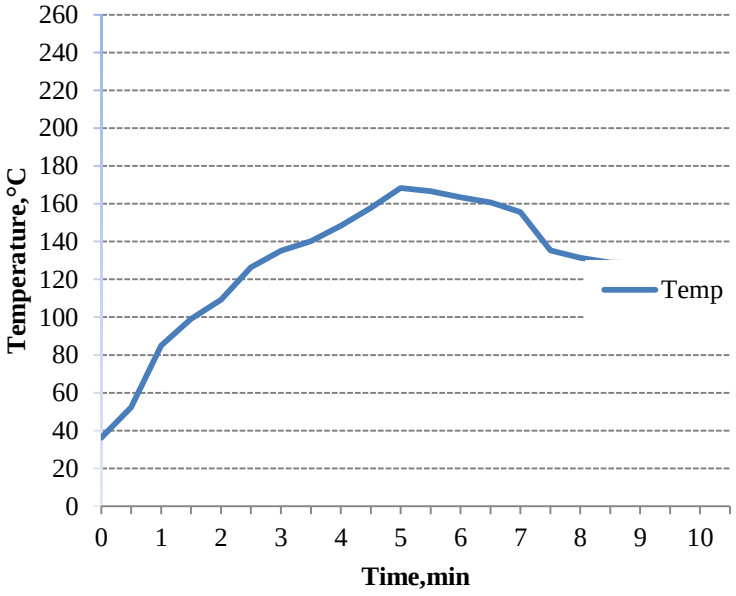

Figure 5.4: Temperature vs. time graph for specimen no 4

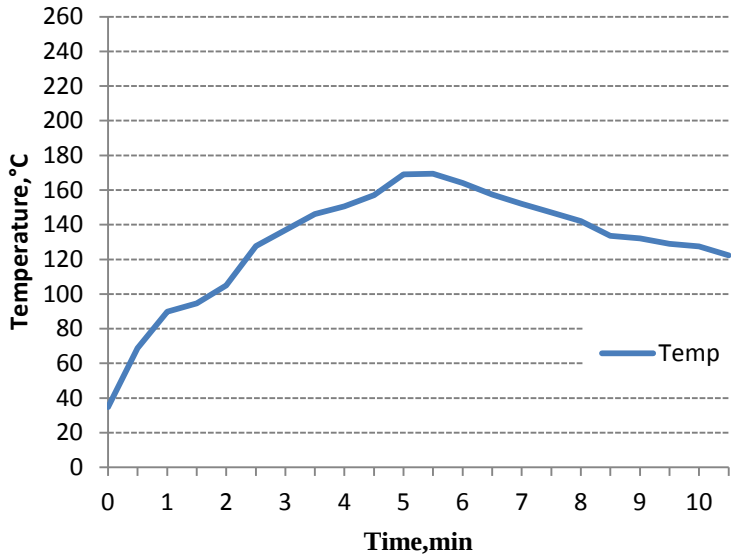

Figure 5.5: Temperature vs. time graph for specimen no 5

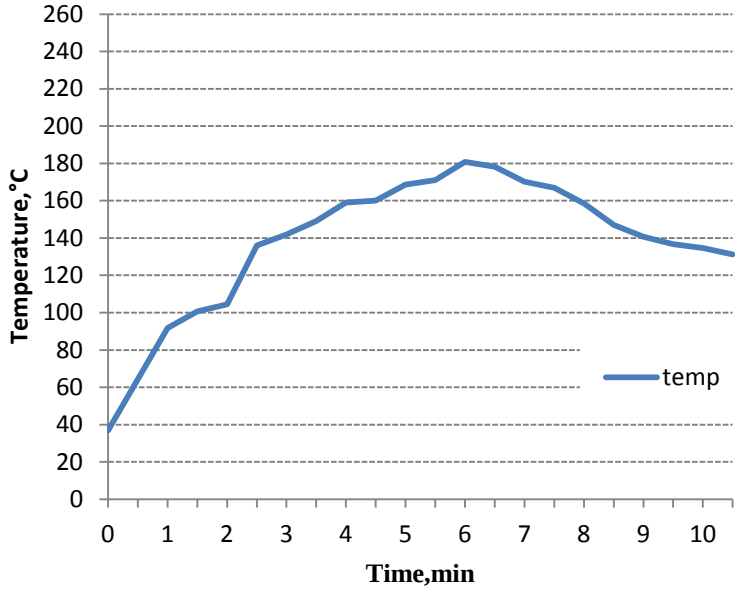

Figure 5.6: Temperature vs. time graph for specimen no 6

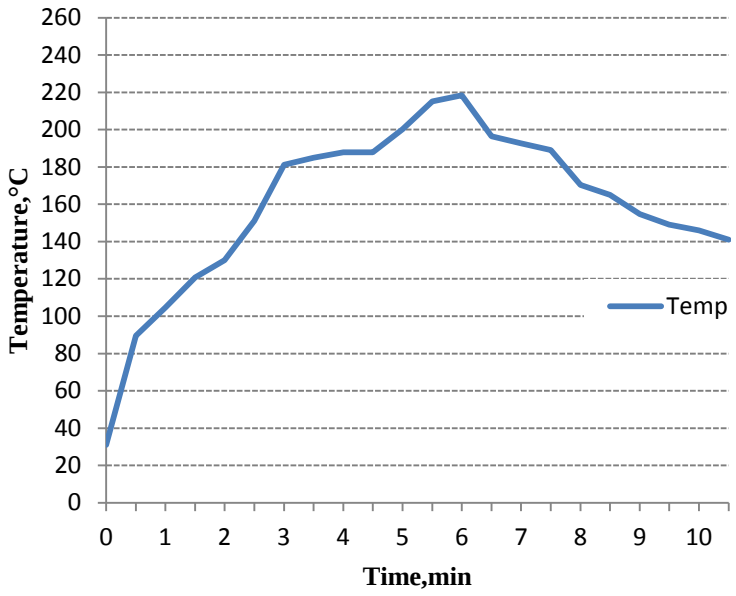

Figure 5.7: Temperature vs. time graph for specimen no 7

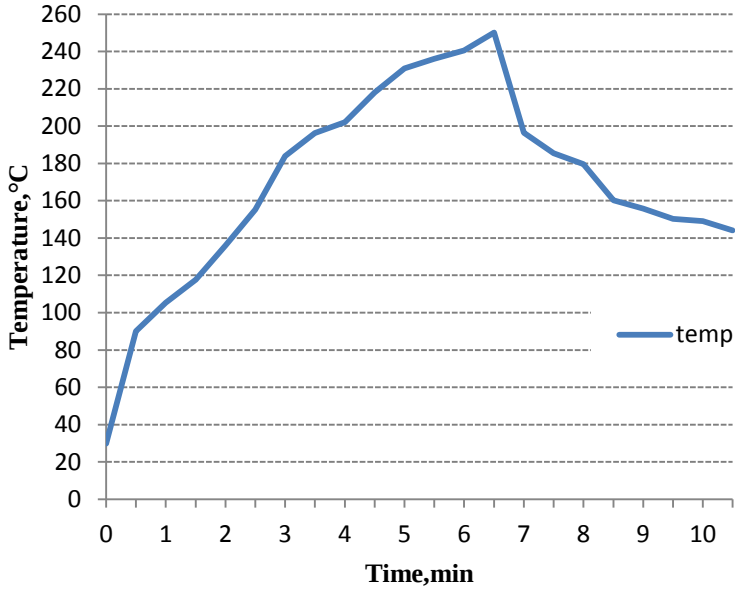

Figure 5.8: Temperature vs. time graph for specimen no 8

Figure 5.9: Temperature vs. time graph for specimen no 9

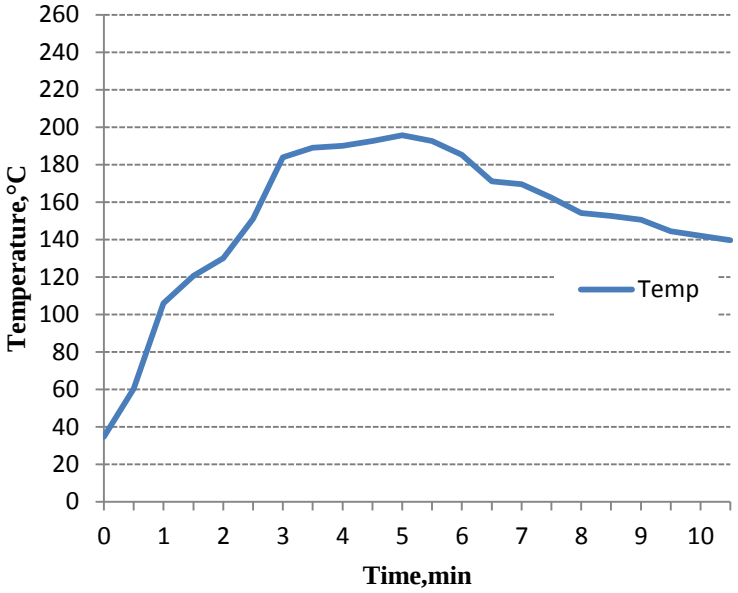

Figure 5.10: Temperature vs. time graph for specimen no 10

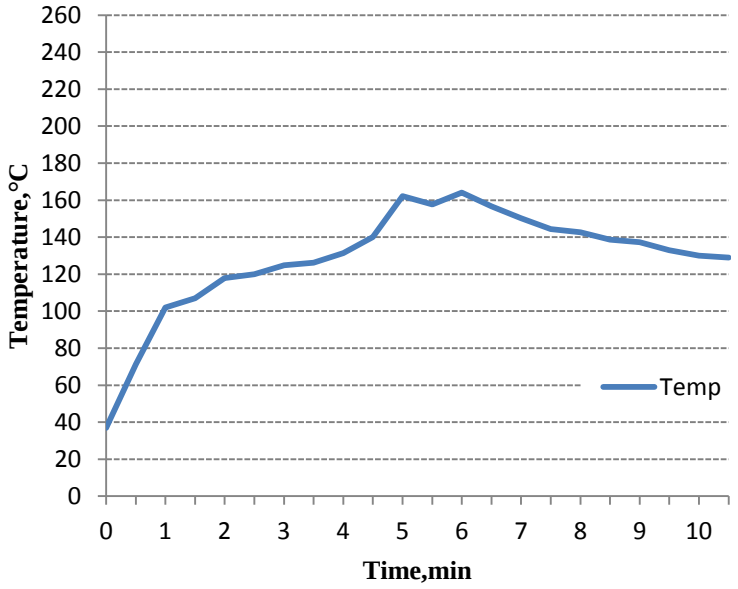

Figure 5.11: Temperature vs. time graph for specimen no 11

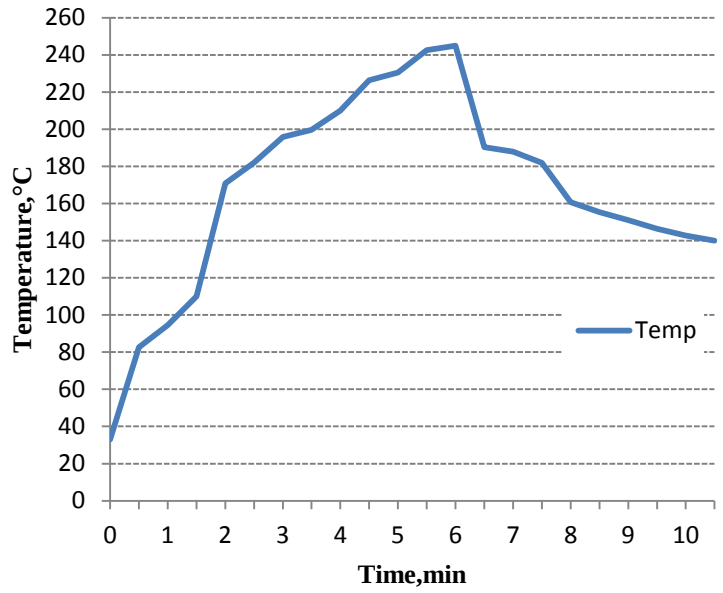

Figure 5.12: Temperature vs. time graph for specimen no 12

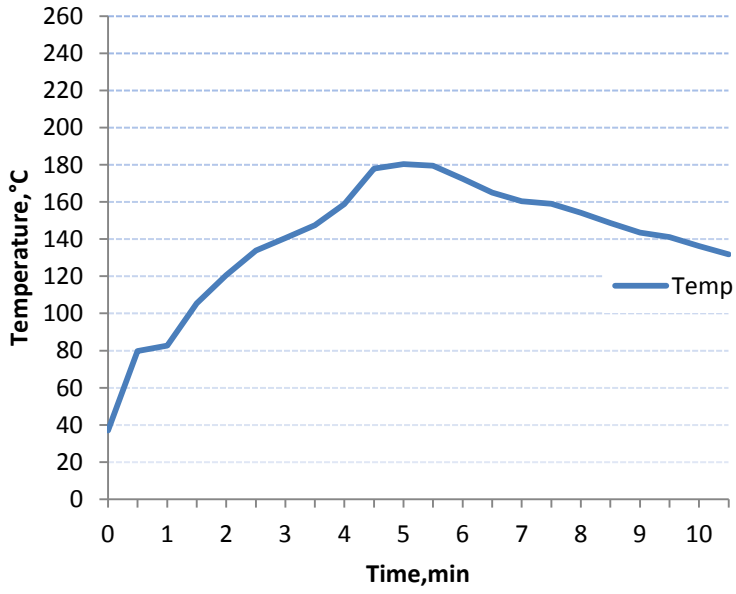

Figure 5.13: Temperature vs. time graph for specimen no 13

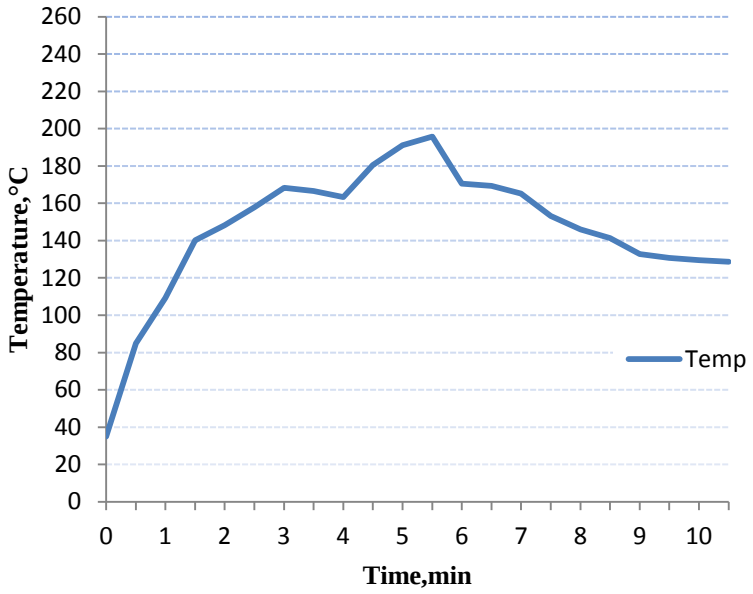

Figure 5.14: Temperature vs. time graph for specimen no 14

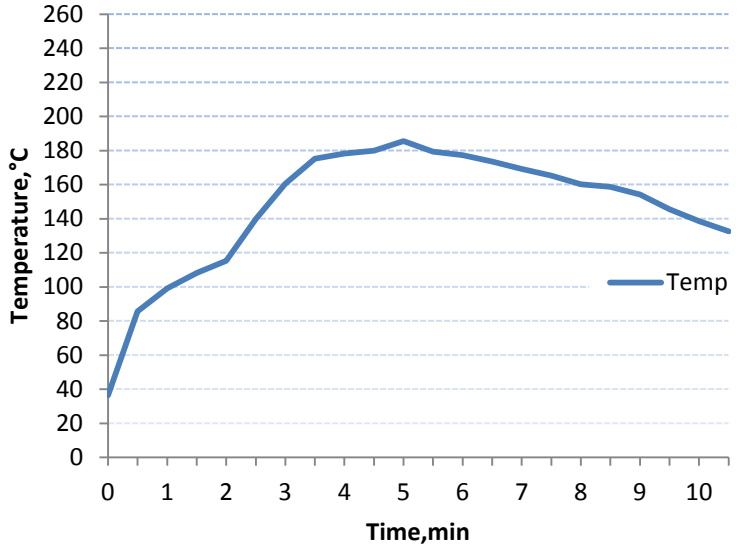

Figure 5.15: Temperature vs. time graph for specimen no 15

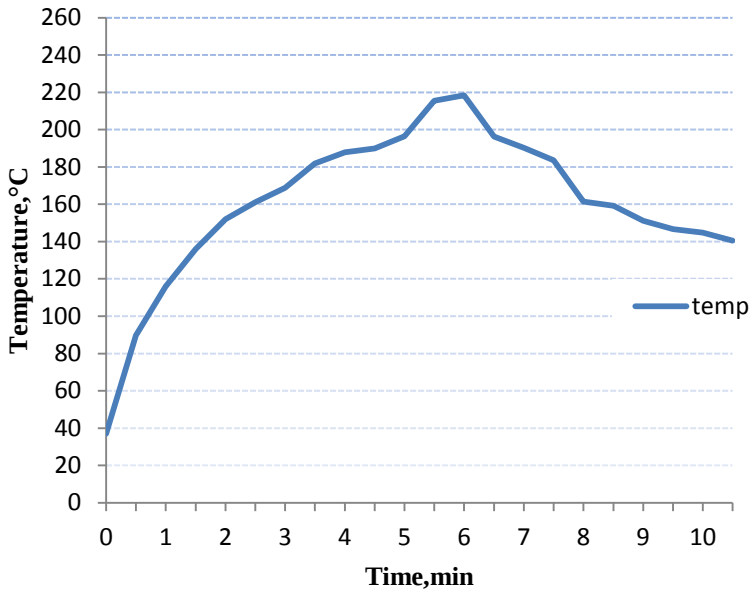

Figure 5.16: Temperature vs. time graph for specimen no 16

5.2.1 Reasons for Temperature Variation:

The heat up and quench rates vary directly with the welding speed while peak temperature is a nonlinear function of the weld power. Peak temperature in the nugget zone depends primarily on weld power; higher the weld power leads to higher temperature for a constant welding speed. Higher power at constant welding speed is obtained by increasing rpm. The highest temperature attained among all the welded plates was 251.4°C at the welding speed of 31.5mm/min and 1800 rpm.

5.3 ULTIMATE TENSILE STRENGTH:

Following table 5.2 and graphs shows the results of tensile strength conducted on Universal testing machine.

Number of Experiments	Parameters				UTM Results		
Sample Number	Tool RPM	Tool Tilt	Plunge D	Traverse Speed	UTS(N/mm^2)	UTL(kN)	Percentage Elongation
1	1120	1	6	16	92.46	11.57	1.87
2	1800	1	6	16	107.59	12.91	3.12
3	1120	2	6	16	122.43	14.69	2.5
4	1800	2	6	16	137.27	16.47	5.07
5	1120	1	10	16	103	12.47	3
6	1800	1	10	16	89.04	10.68	1.81
7	1120	2	10	16	126.14	15.14	2.37
8	1800	2	10	16	120.04	13.8	3.56

9	1120	1	6	31.5	92.75	11.13	1.75
10	1800	1	6	31.5	105.74	12.69	3.5
11	1120	2	6	31.5	115.01	13.8	3.56
12	1800	2	6	31.5	118.72	14.25	2.75
13	1120	1	10	31.5	100	12.02	2.9
14	1800	1	10	31.5	130.59	15.67	4.18
15	1120	2	10	31.5	129.85	15.58	3.75
16	1800	2	10	31.5	133.56	16.03	4.37
Base material					111.30	13.36	9.09

Table 5.1 Test matrix for UTM results

Following are the plots of load vs displacement for welds made different welding speeds.

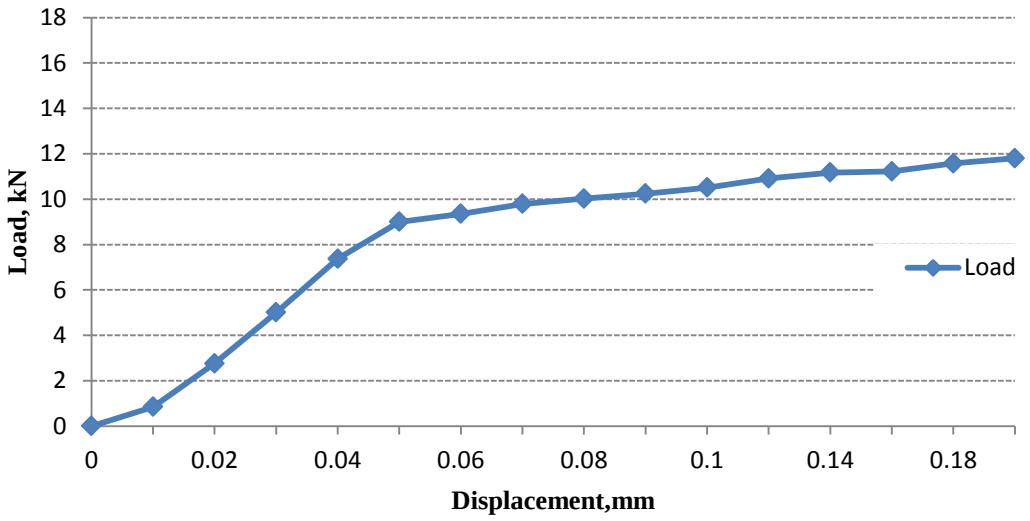

Figure 5.17: Load vs. displacement graph for specimen no 1

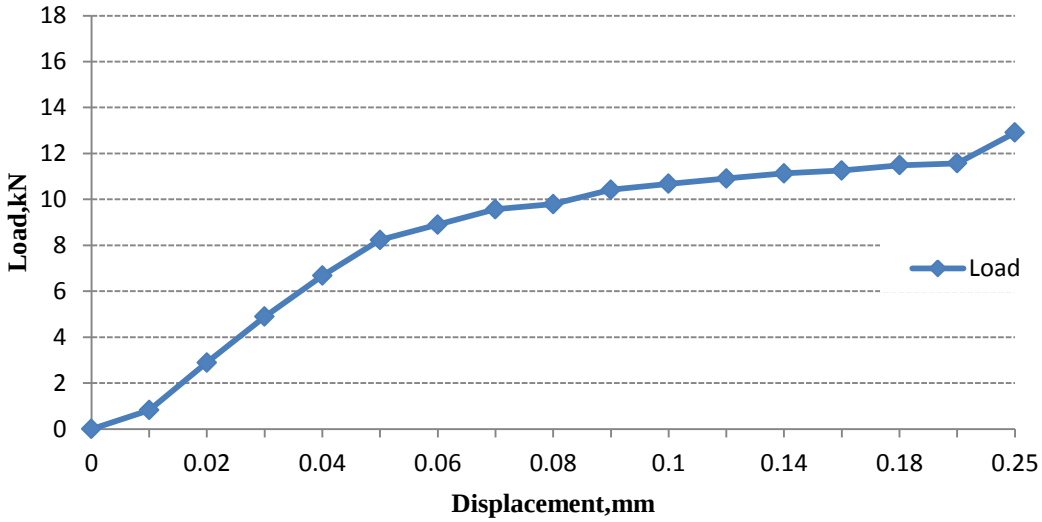

Figure 5.18: Load vs. displacement graph for specimen no 2

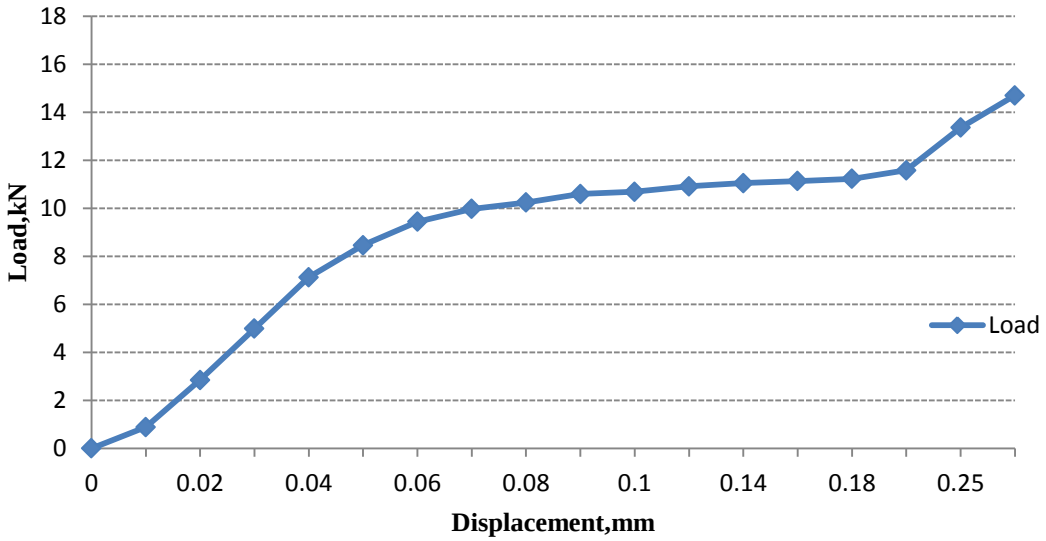

Figure 5.19 Load vs. displacement graph for specimen no 3

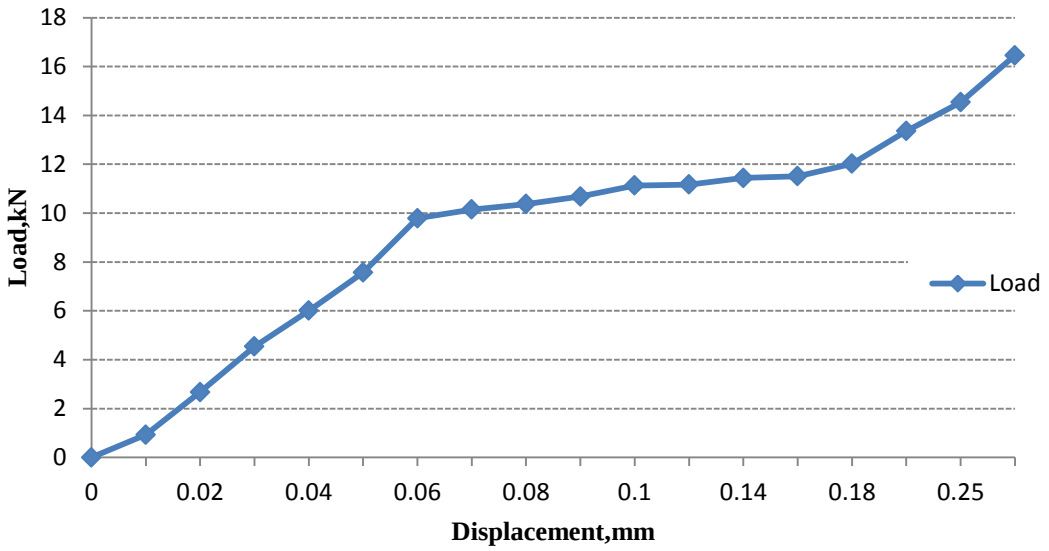

Figure 5.20: Load vs. displacement graph for specimen no 4

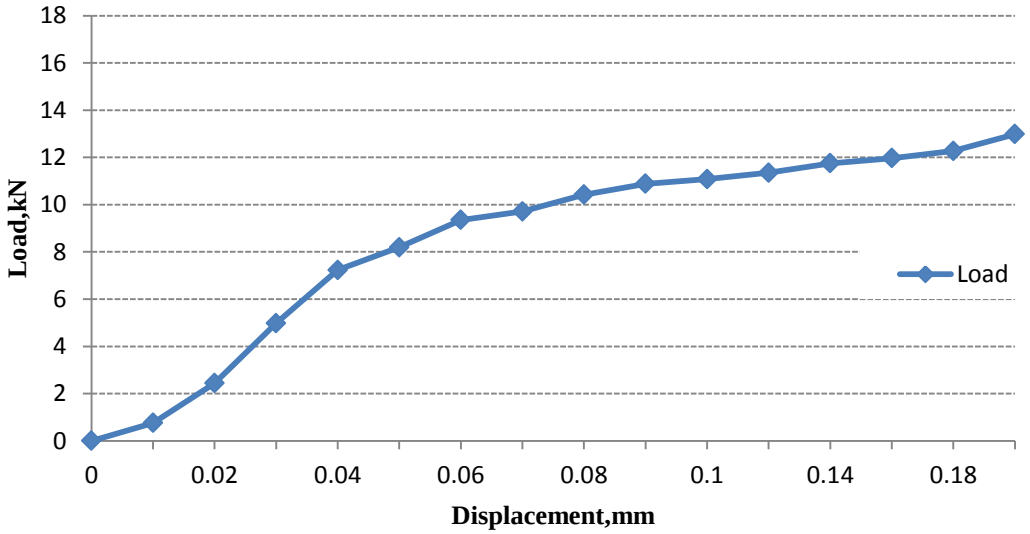

Figure 5.21: Load vs. displacement graph for specimen no 5

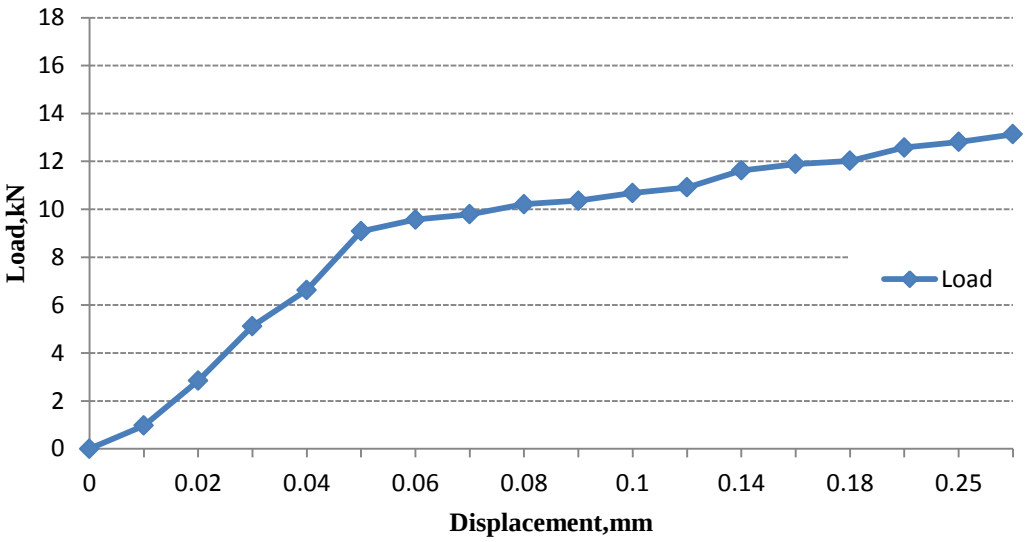

Figure 5.22 Load vs. displacement graph for specimen no 6

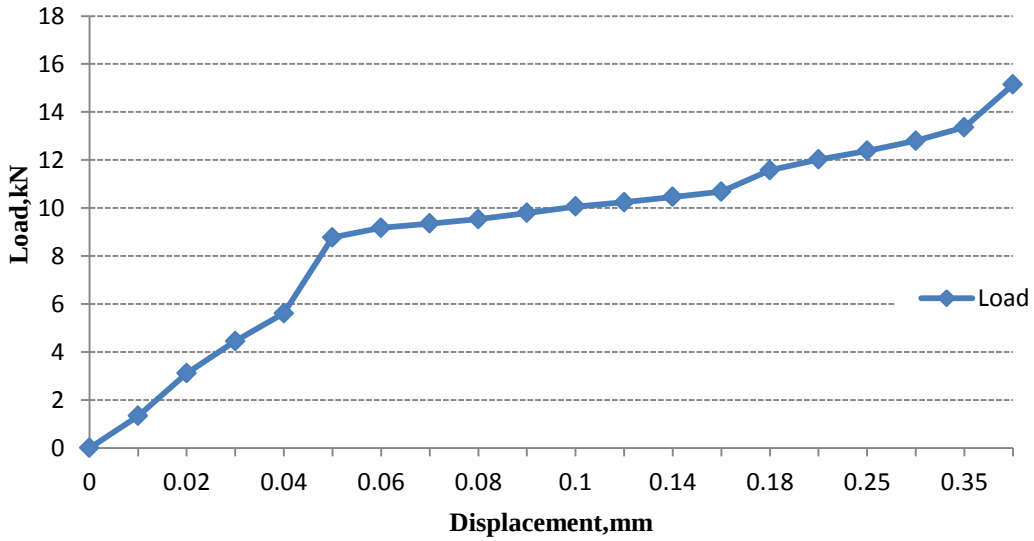

Figure 5.23: Load vs. displacement graph for specimen no 7

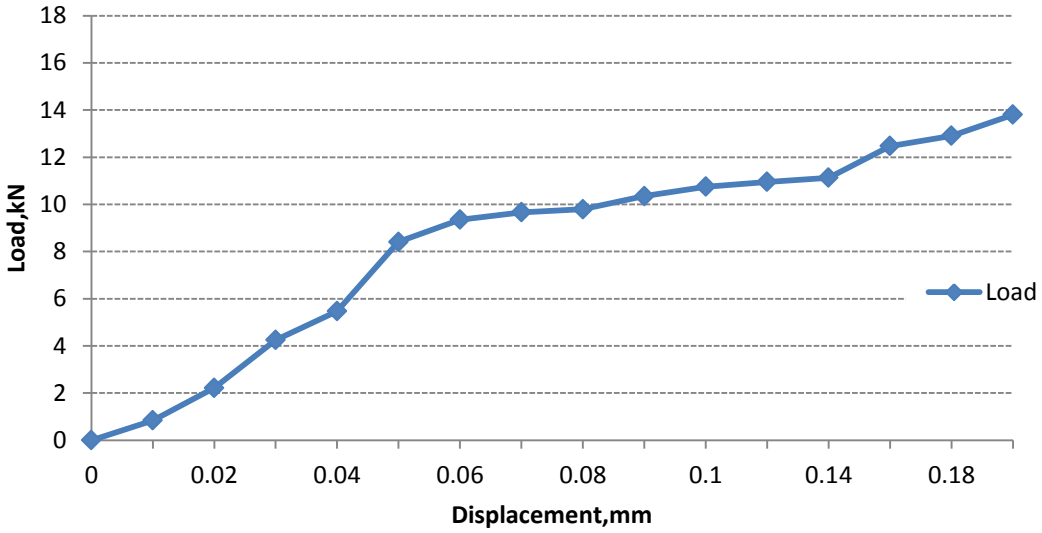

Figure 5.24: Load vs. displacement graph for specimen no 8

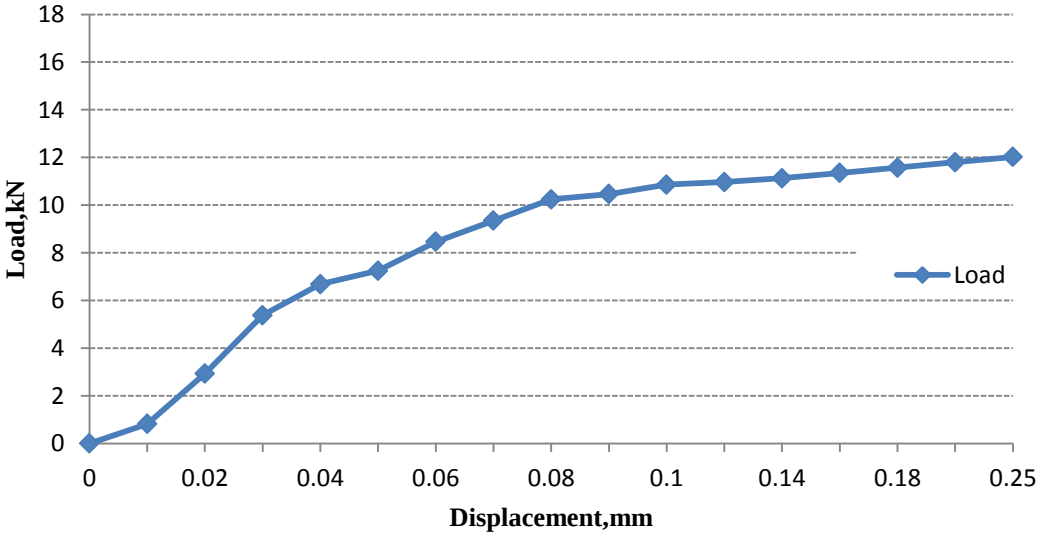

Figure 5.25: Load vs. displacement graph for specimen no 9

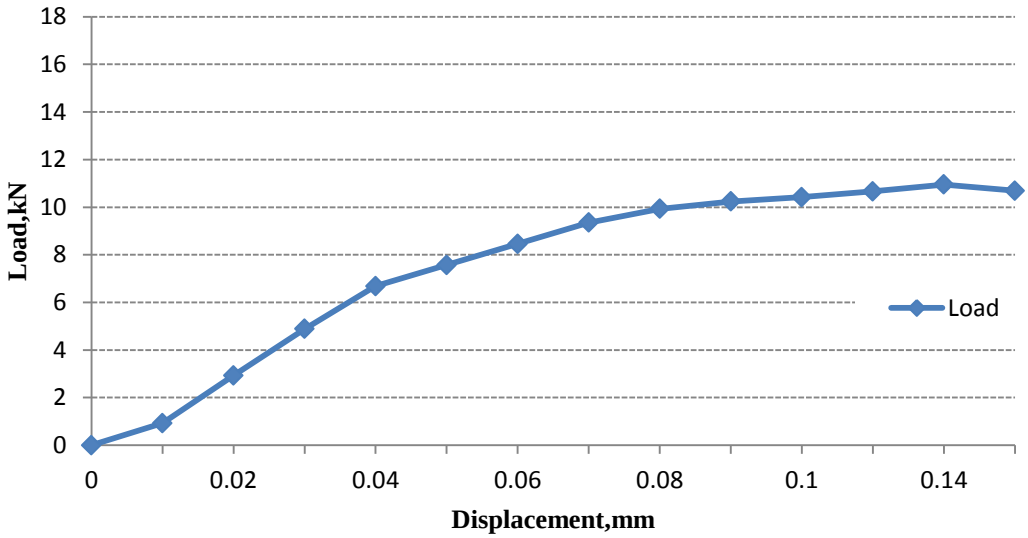

Figure 5.26: Load vs. displacement graph for specimen no 10

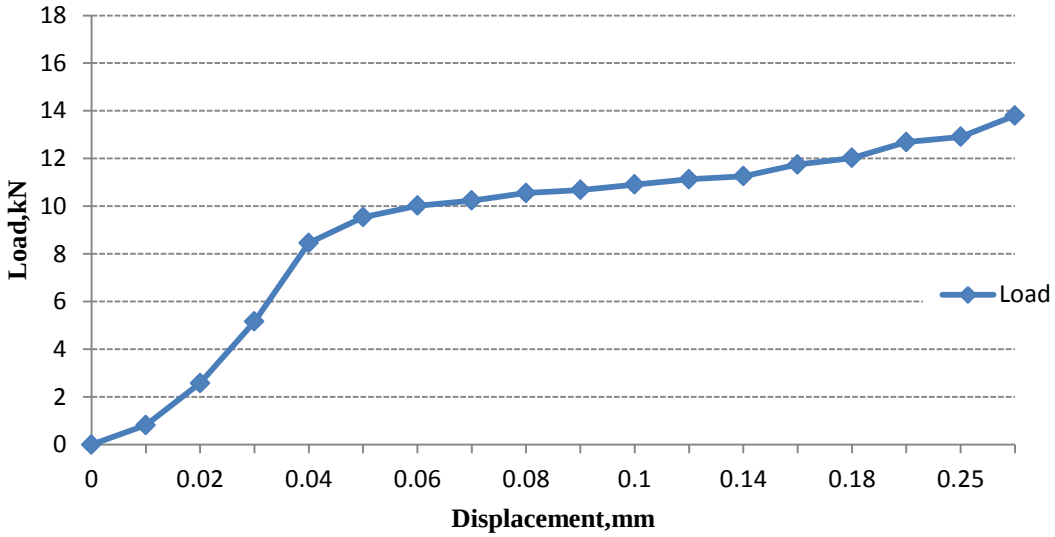

Figure 5.27: Load vs. displacement graph for specimen no 11

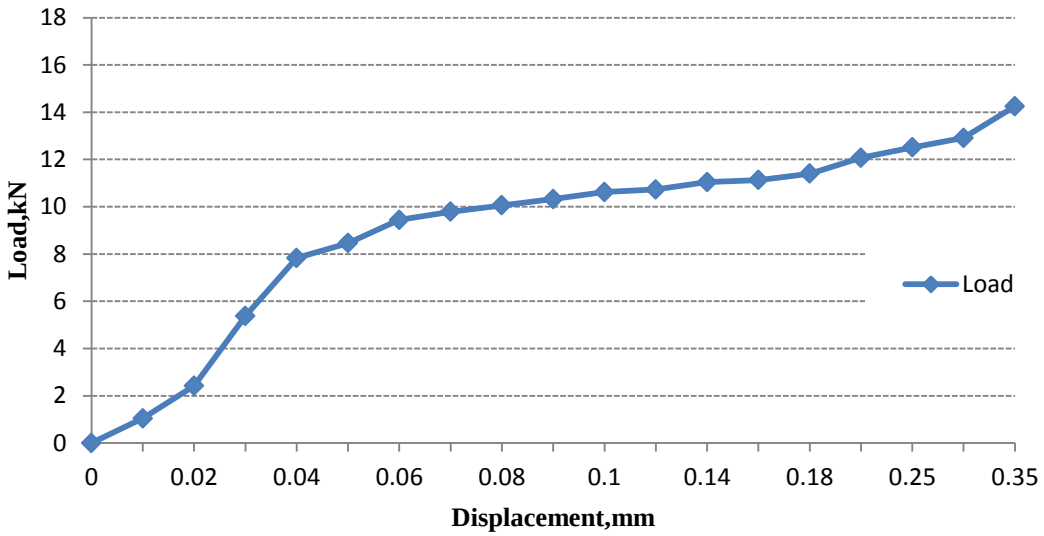

Figure 5.28: Load vs. displacement graph for specimen no 12

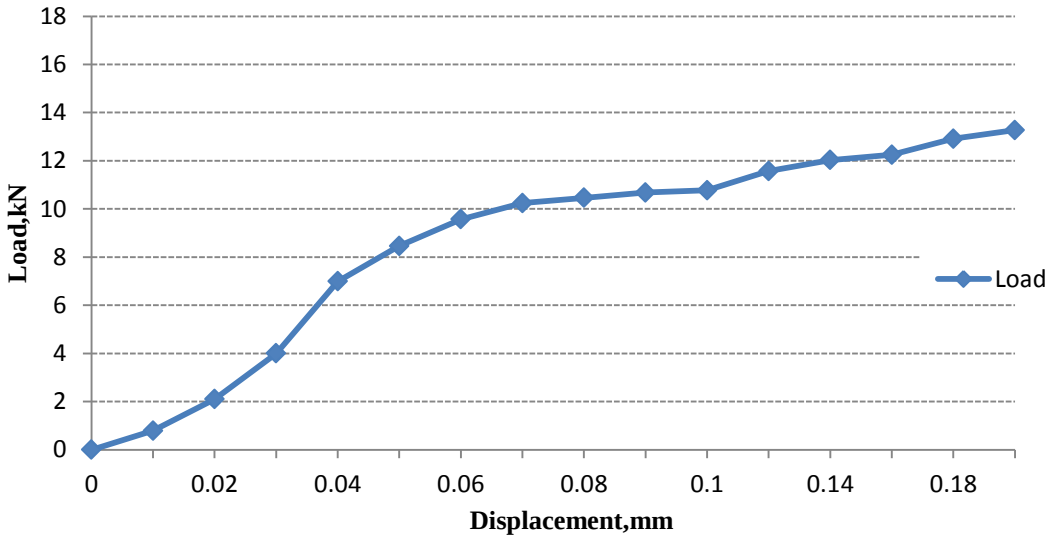

Figure 5.29: Load vs. displacement graph for specimen no 13

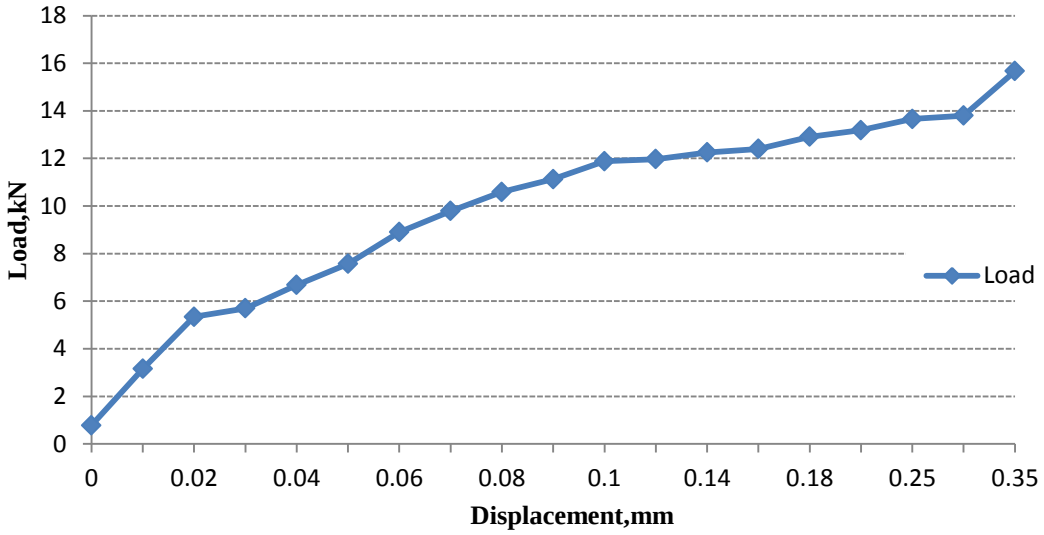

Figure 5.30: Load vs. displacement graph for specimen no 14

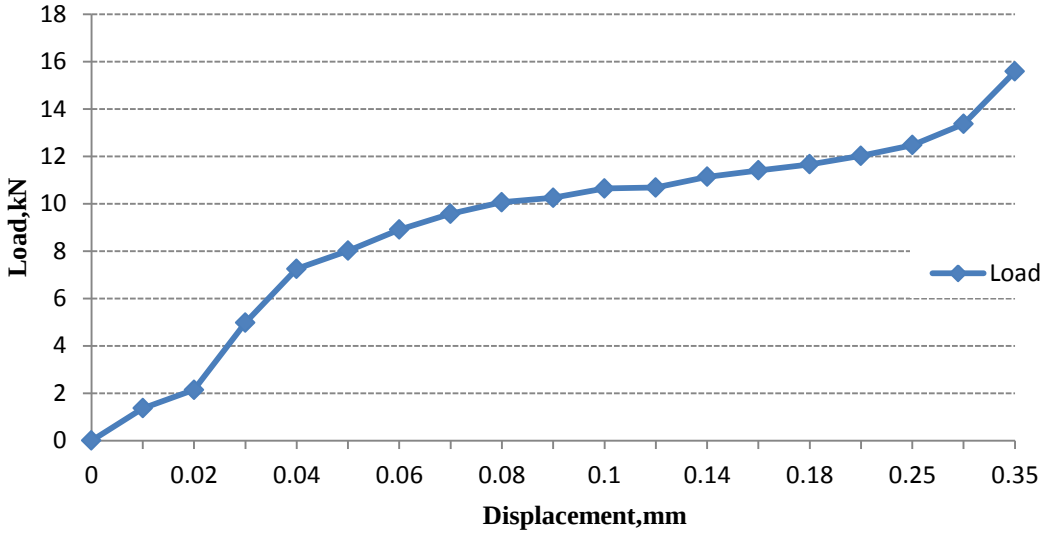

Figure 5.31: Load vs. displacement graph for specimen no 15

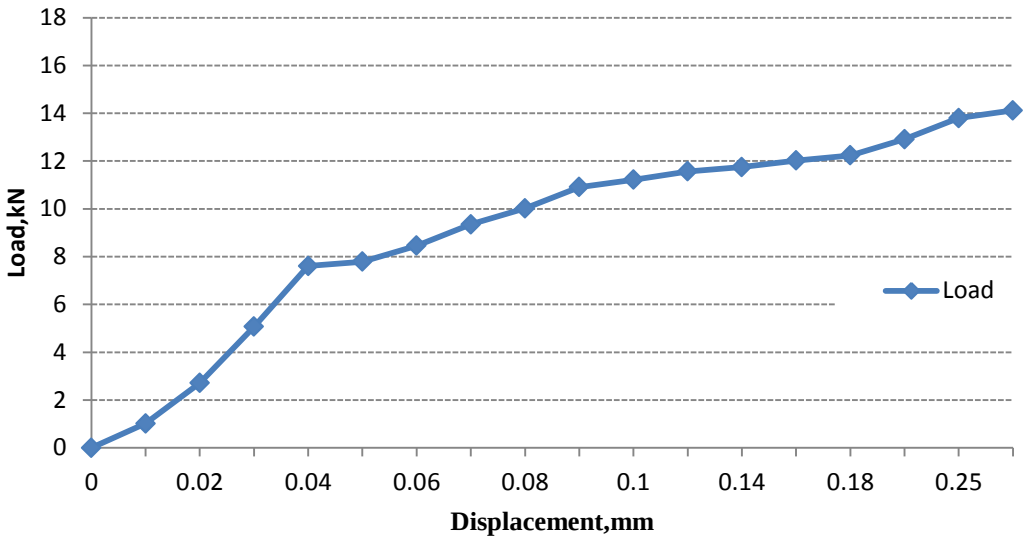

Figure 5.32: Load vs. displacement graph for specimen no 16

5.3.1 Reasons for Tensile Strength Variations:

Increase in rotational speed has resulted in increase of tensile strength. The reason is that higher the speed, higher will be the deformation and heat generated in the weld. This will result in finer grain structure because of which tensile strength increases. Maximum tensile strength obtained at welding speed 1800 rpm and 31.5mm/min traverse speed was 133.56 N/mm^2. Where as minimum value i.e. 92.46 N/mm^2 was obtained at welding speed 1120 rpm and 16 mm/min traverse speed.

Some samples failed at lower loads than the anticipated value for the base material. This is a result of unequal strain distribution across the sample resulting from the heterogeneous properties of the weld. The other reason may could be, that the local strains may have reached close to the expected bulk strain. Figure5.33 shows the fracture point of specimen during tensile testing.

Figure 5.33: Sample fractured in tensile testing.

5.4 ROCKWELL HARDNESS TEST

Following table and graph shows the surface hardness (HRB) at friction stir weld, between stir zone, heat-affected zone and parent material.

Sample Number	Distance from weld centre line, mm						
	-30	- 20	-10	Weld line	10	20	30
1	74	75	76,	71.7	75	76.8	76
2	73	74	76	75	79	77.5	76
3	74.5	73	74	74	76	78	75
4	76.5	74	72	75	73.8	73	73.5
5	80	82	75	77	74	78	81
6	76	75	73	75.5	70	76	78
7	72	73.5	74	70	73.8	73	72
8	77	80	75	76	72	83.5	79
9	78	81	76	73.8	71	79	80
10	74	75	75	78	71	76	74
11	79.6	78	74	69	70	78.5	79
12	75	70	72	73.6	72.6	72	77
13	74	78.7	77	75	78	75.5	74
14	80.2	74	75.5	77	73	75	79
15	81	79	78.3	74	75	80	82
16	76.8	74	75	74	71.4	74	76.6

Table5.3: Test matrix for Hardness test

Following 16 graphs show the variation of surface hardness at centre of weld and various distances at various welds for all welded samples:

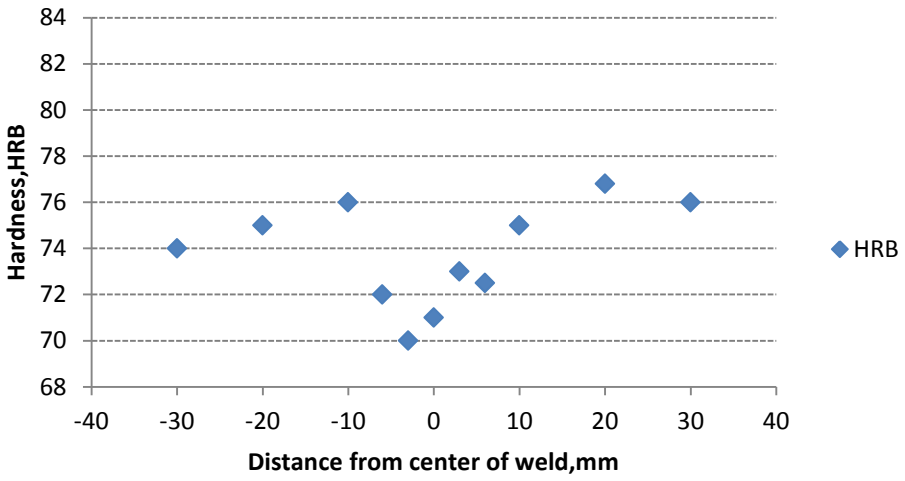

Figure 5.34: Hardness curve for specimen no 1

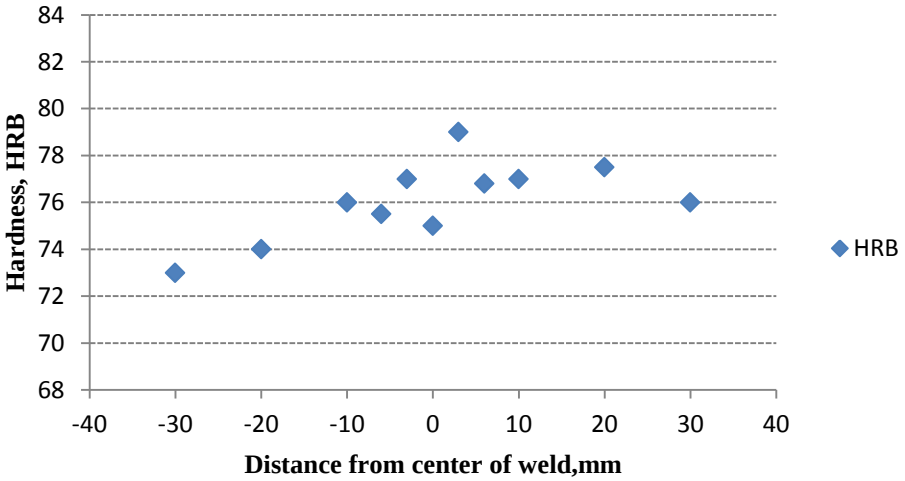

Figure 5.35: Hardness curve for specimen no 2

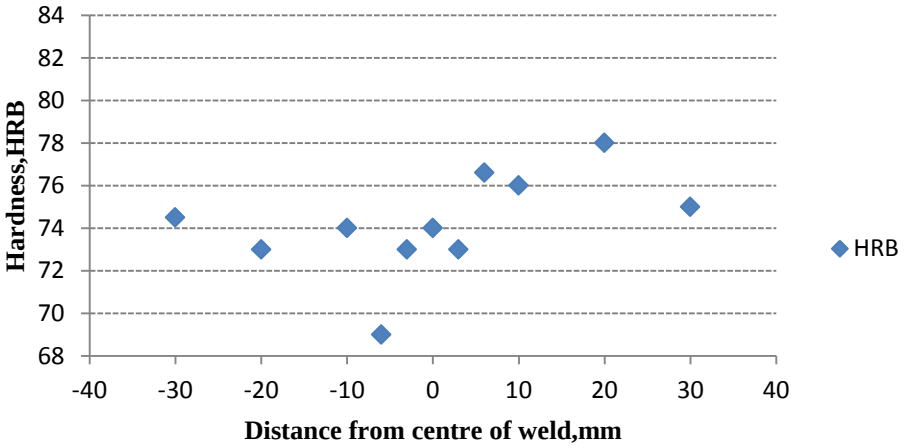

Figure 5.36: Hardness curve for specimen no 3

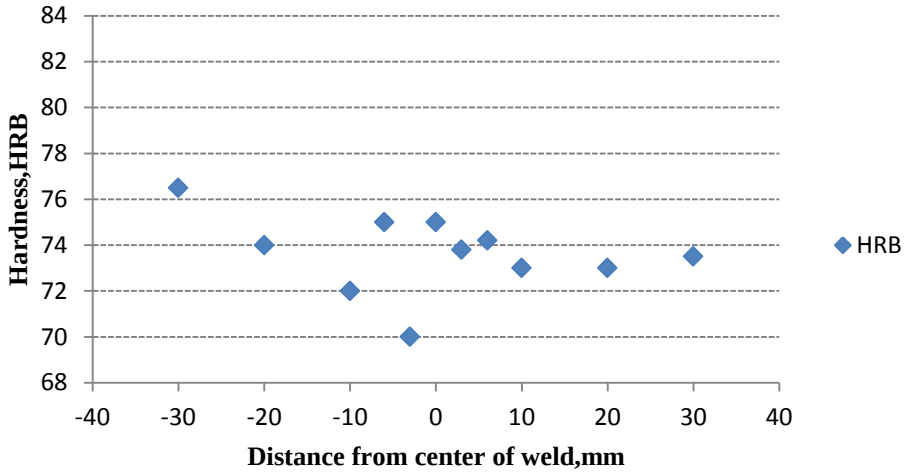

Figure 5.37: Hardness curve for specimen no 4

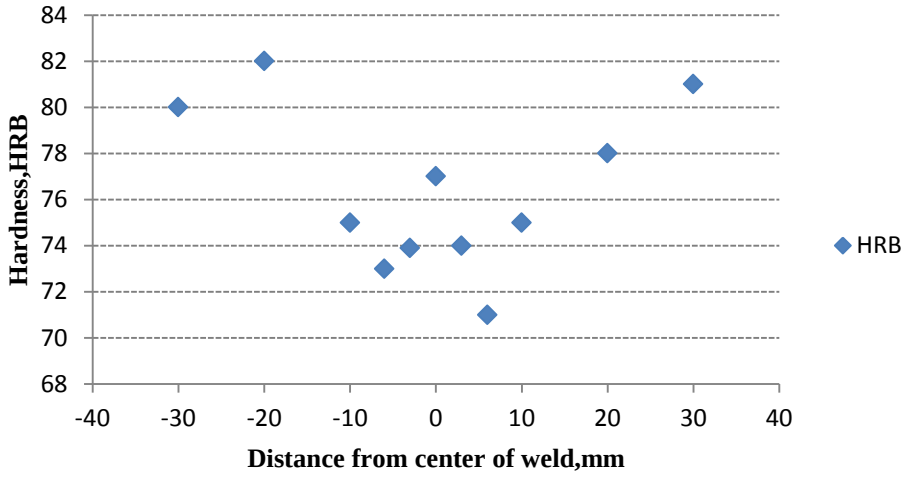

Figure 5.38: Hardness curve for specimen no 5

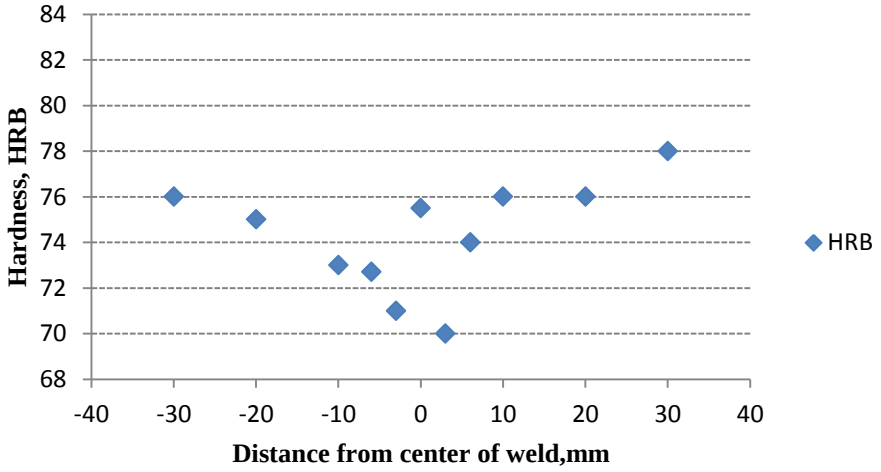

Figure 5.39: Hardness curve for specimen no 6

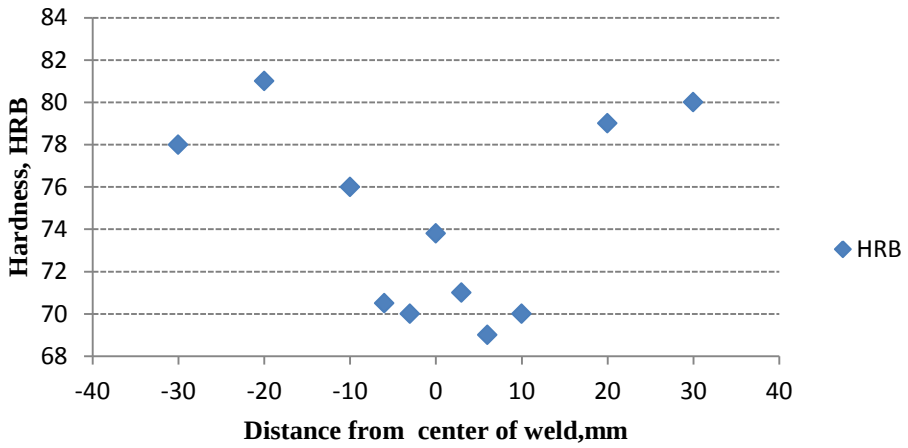

Figure 5.40: Hardness curve for specimen no 7

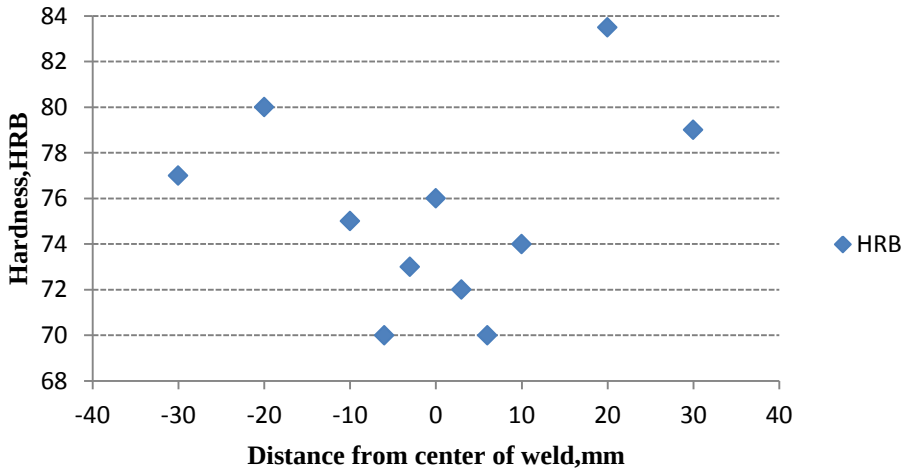

Figure 5.41: Hardness curve for specimen no 8

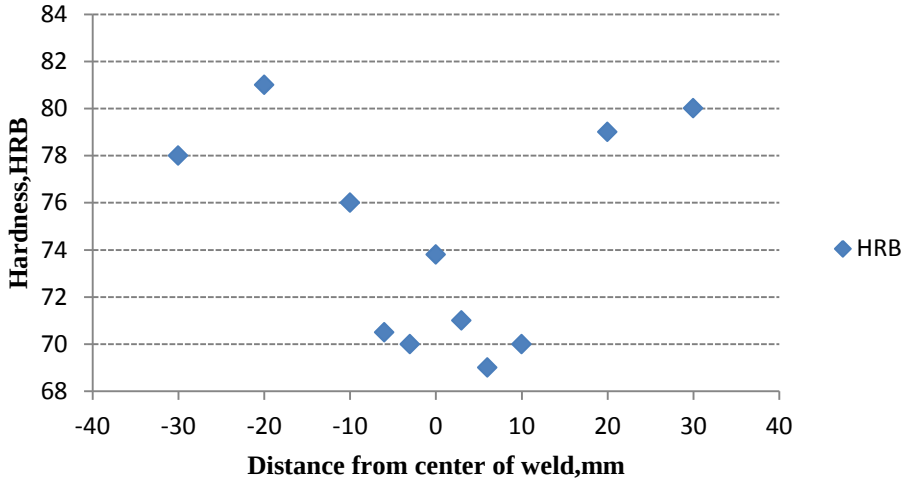

Figure 5.42: Hardness curve for specimen no 9

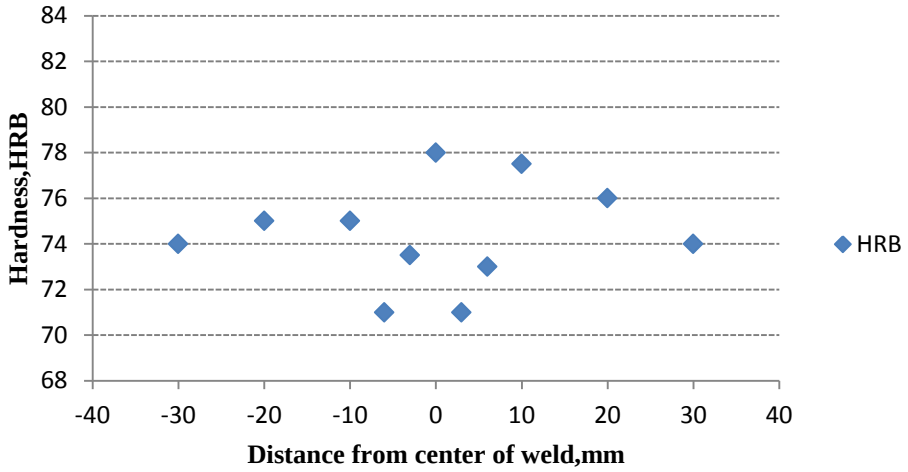

Figure 5.43: Hardness curve for specimen no 10

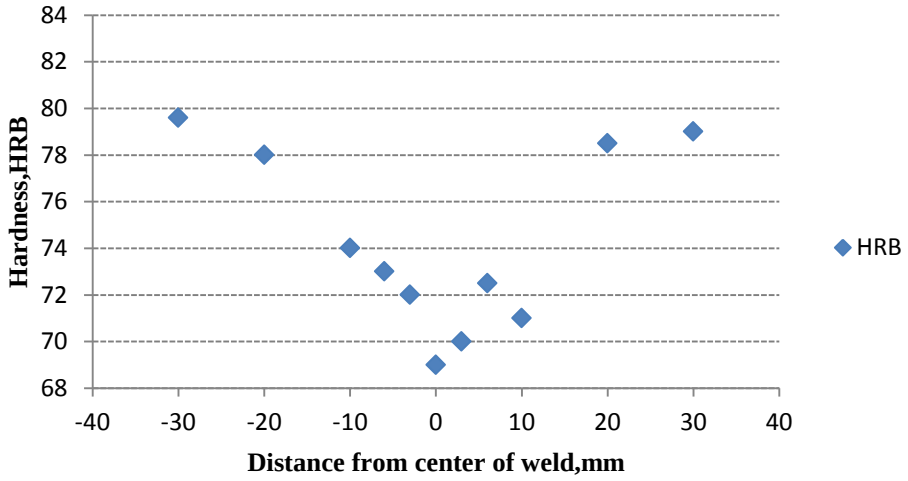

Figure 5.44: Hardness curve for specimen no 11

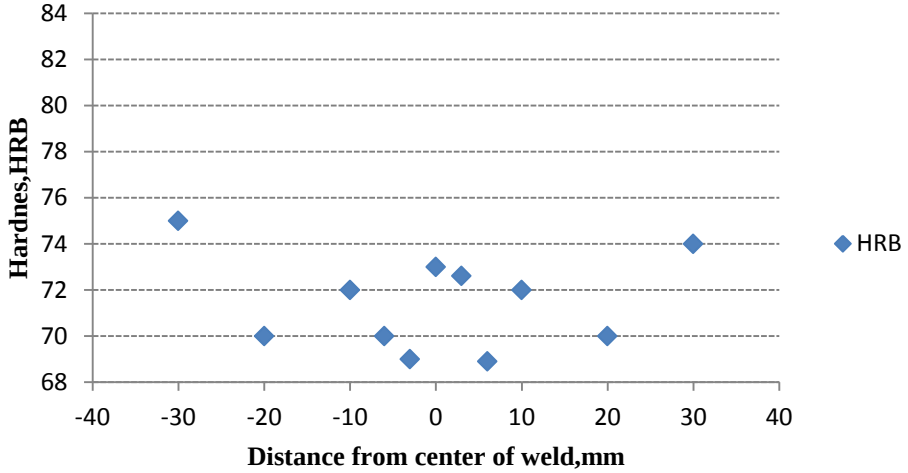

Figure 5.45: Hardness curve for specimen no 12

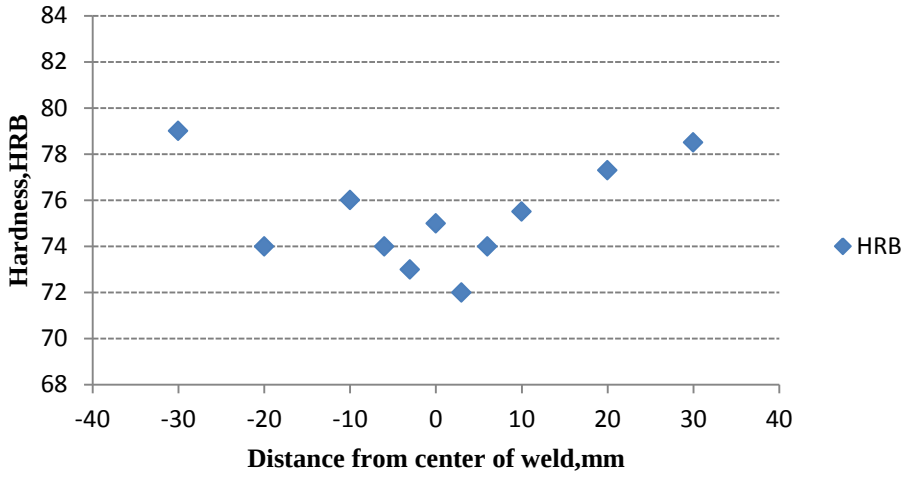

Figure 5.46: Hardness curve for specimen no 13

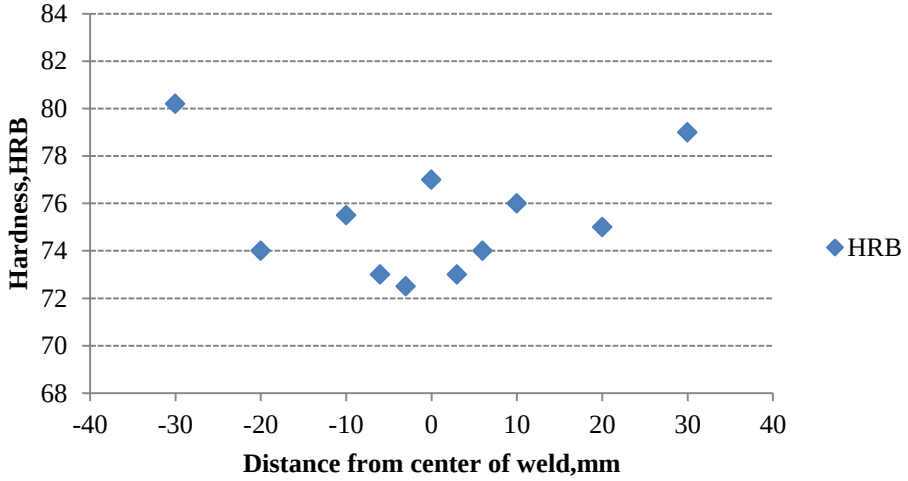

Figure 5.47: Hardness curve for specimen no 14

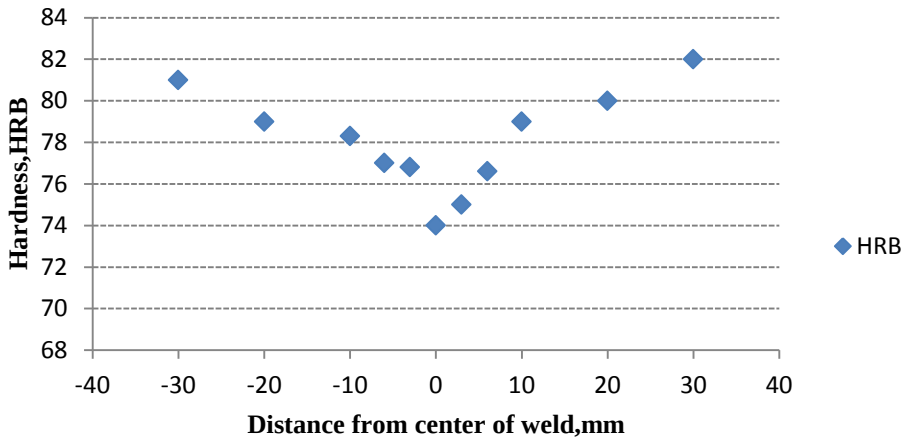

Figure 5.48: Hardness curve for specimen no 15

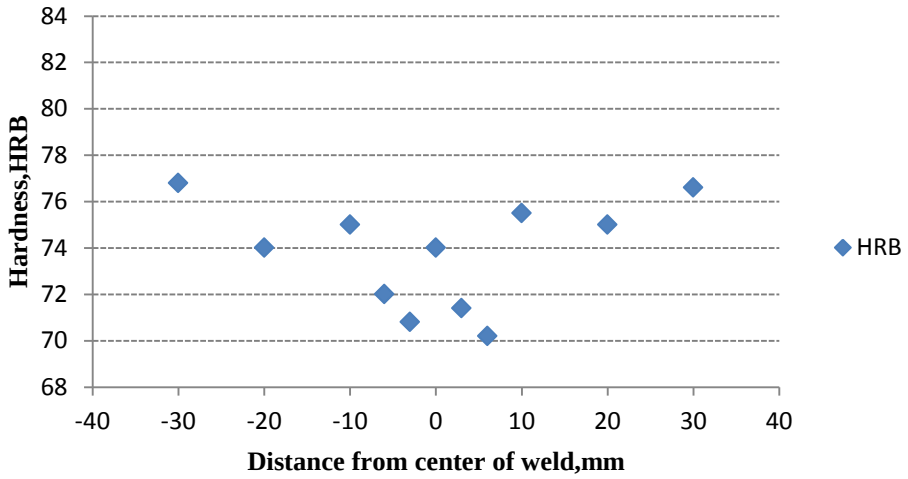

Figure 5.49: Hardness curve for specimen no 16

5.4.1 Reasons for Variation in Rockwell Hardness:

Hardness is a function of both distance from the joint surface as well tool depth.

As shown in above figures, a typical "W-shaped" hardness curved is created for some specimens. The reasons for the four distinct hardness zones are:

- The weld nugget extending 5 to mm from each side of the joint interface, where hardness is nearly constant.
- The remainder of the TMAZ extending from 5 to 6mm from the weld nugget, where hardness decreases.
- The HAZ extending an additional 15-20mm from TMAZ, where hardness

reaches a minimum and then increases as distance from the weld centerline increases, in some cases even achieving hardness greater than that of parent material.

- The hardness of HAZ is dependent primarily on the welding speed ; higher welding speed corresponds to higher HAZ hardness.
- The hardness of parent material is unaffected by FSW.

5.5 IZOD IMPACT TEST

Izod impact was performed on three samples of each welded plate for checking the accuracy. Following table and graph indicates the results of test performed.

Number of Experiments	Parameters				Impact Value, Joule		
Sample Number	Tool RPM	Tool Tilt	Plunge D	Traverse Speed	Test 1	Test 2	Test 3
1	1120	1	6	16	26	25	28
2	1800	1	6	16	45	40	41
3	1120	2	6	16	40	38	37
4	1800	2	6	16	26	36	36
5	1120	1	10	16	28	30	31
6	1800	1	10	16	43	42	41
7	1120	2	10	16	26	26	31
8	1800	2	10	16	38	36.2	38
9	1120	1	6	31.5	36	32.5	33
10	1800	1	6	31.5	24	28	30
11	1120	2	6	31.5	38	36	33
12	1800	2	6	31.5	32	38	34
13	1120	1	10	31.5	31	30	32
14	1800	1	10	31.5	44	38	42
15	1120	2	10	31.5	22	28	36
16	1800	2	10	31.5	42	34	42

Table 5.4: Test matrix table for impact test results

Following graphs shows the comparison between all the impact energy obtained for all 18 specimens:

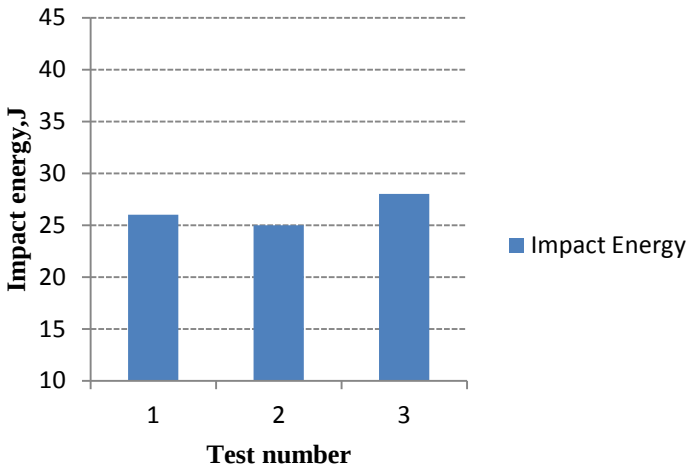

Figure 5.50: Impact energy for specimen no 1

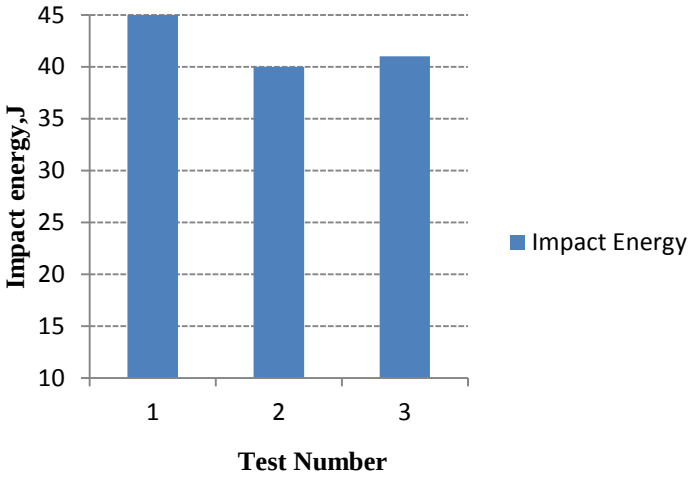

Figure 5.51:Impact energy for specimen no 2

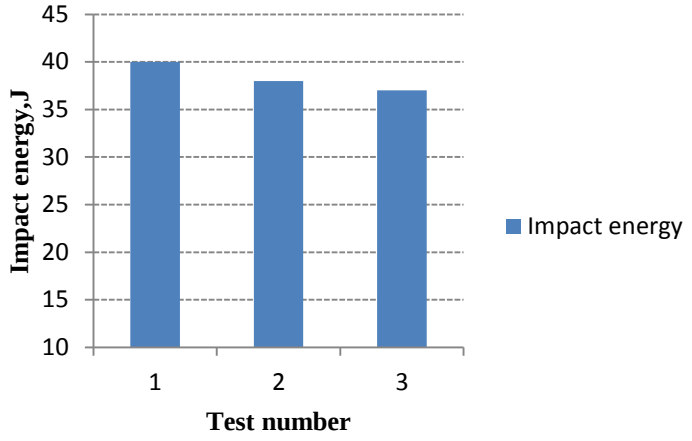

Figure 5.52: Impact energy for specimen no3

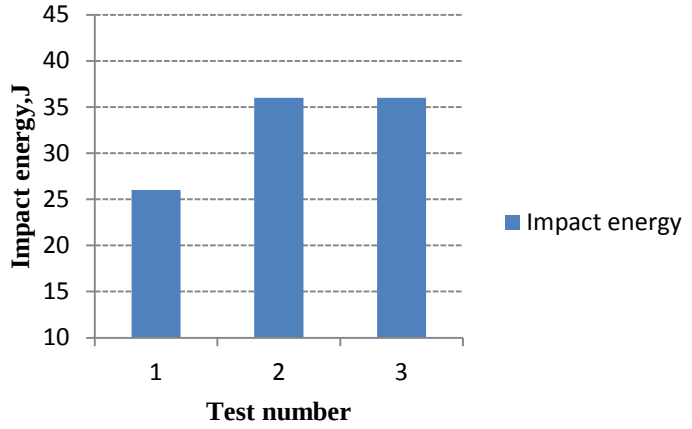

Figure 5.53: Impact energy for specimen no4

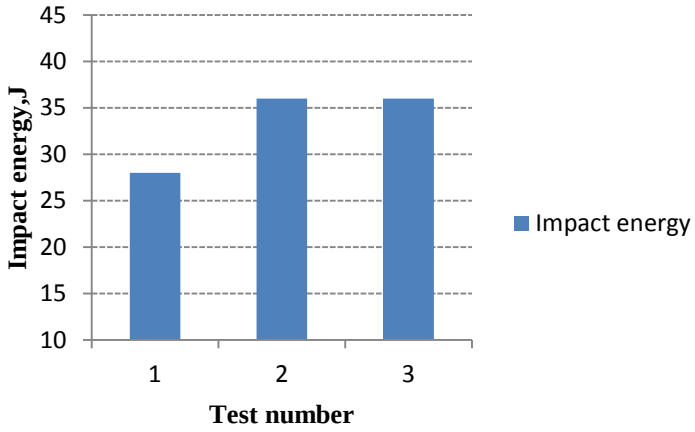

Figure 5.54: Impact energy for specimen no5

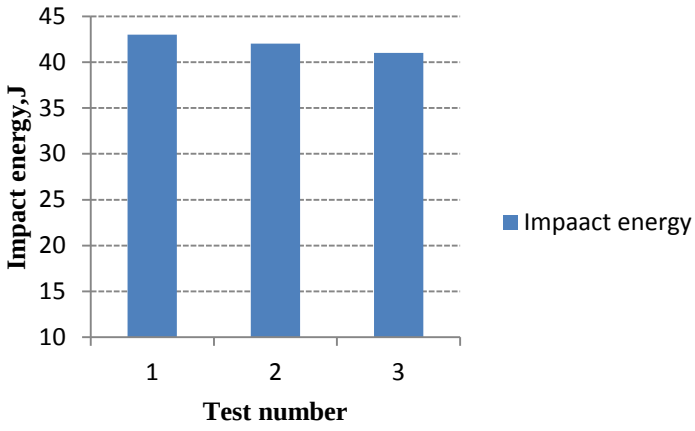

Figure 5.55: Impact energy for specimen no6

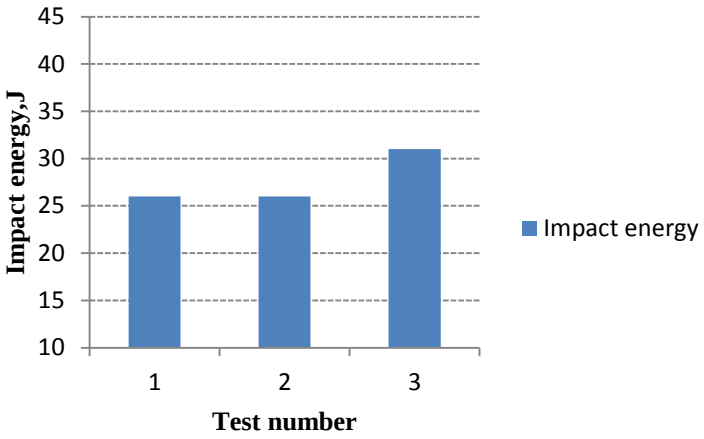

Figure 5.56: Impact energy for specimen no7

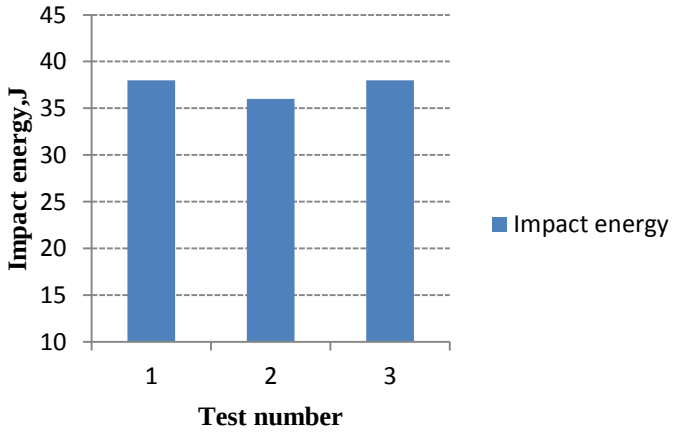

Figure 5.57: Impact energy for specimen no8

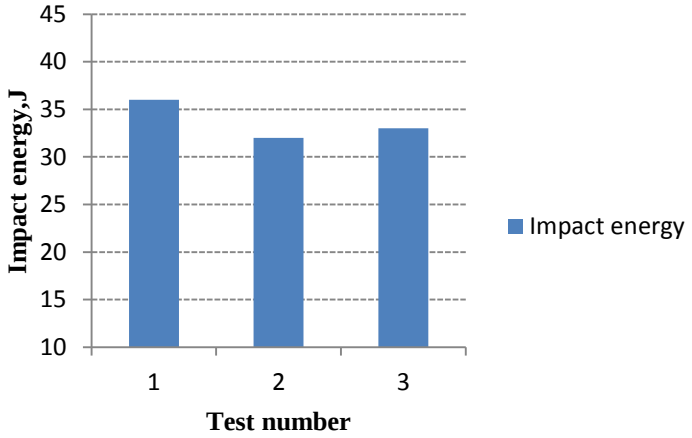

Figure 5.58: Impact energy for specimen no9

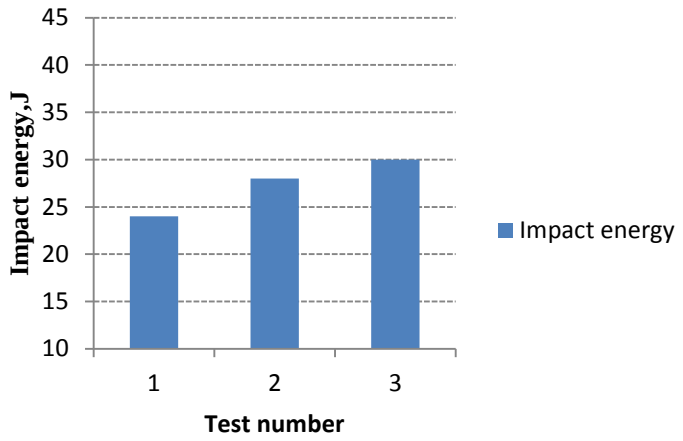

Figure 5.59: Impact energy for specimen no10

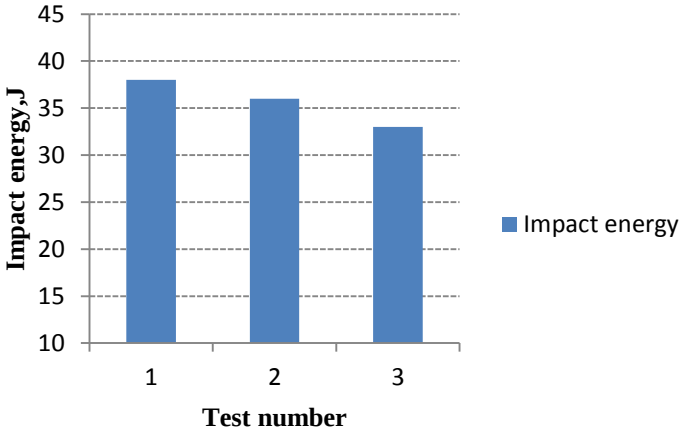

Figure 5.60: Impact energy for specimen no11

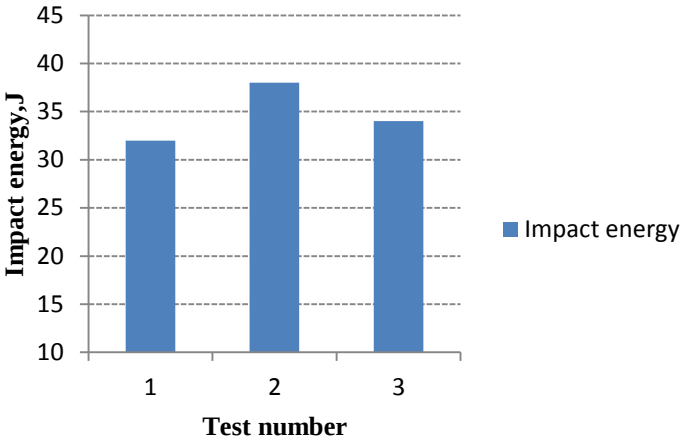

Figure 5.61: Impact energy for specimen no12

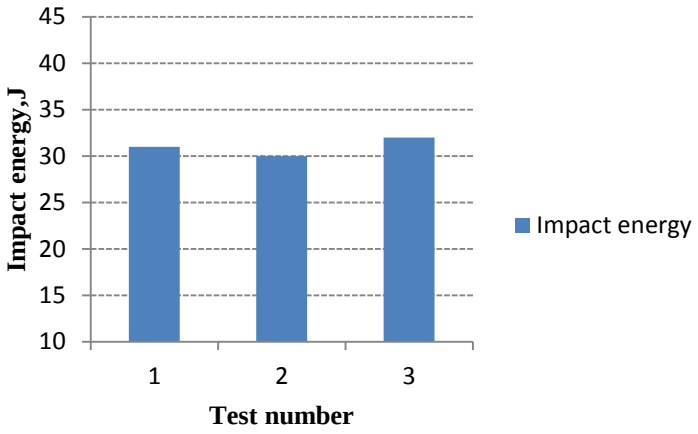

Figure 5.62: Impact energy for specimen no13

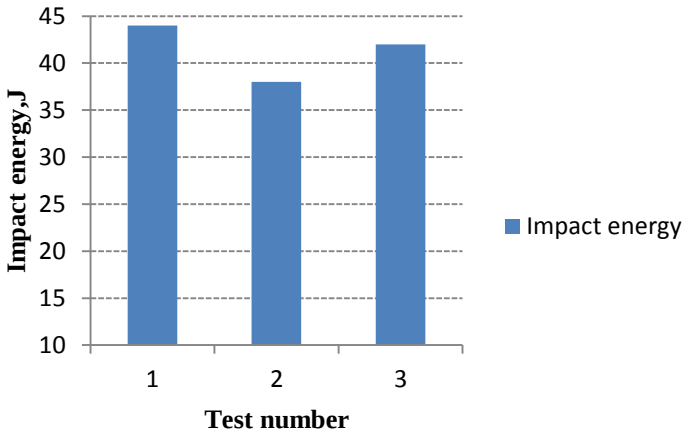

Figure5.63: Impact energy for specimen no14

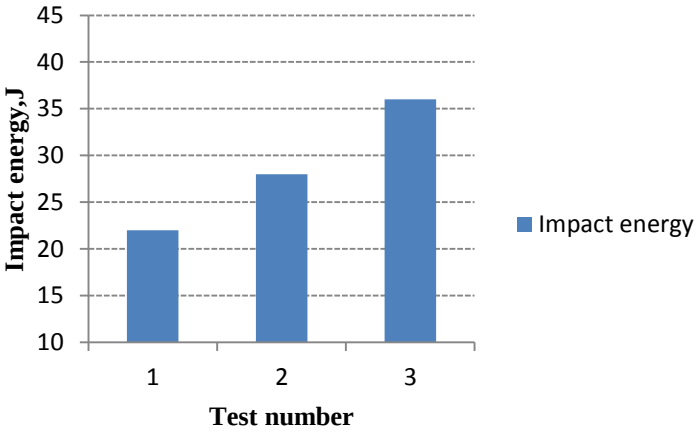

Figure 5.64: Impact energy for specimen no15

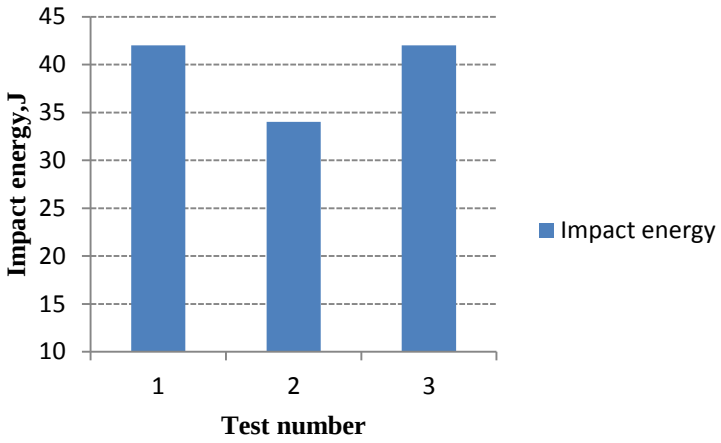

Figure 5.65: Impact energy for specimen no16

5.5.1 Discussion on Impact Test Results

The average value of impact energy can be taken as the average of each sample. From the above table and graphs it can be concluded that impact energy increases with increase in rpm and traverse speed. The highest value of impact energy is 44 Joules at 1800 rpm both for 1° and 2° parameters. Whereas the lowest value is 26 Joule at 1120 rpm.

5.6 MICRO STRUCTURE DEVELOPMENT IN FRICTION STIR WELDS

Following are the optical micrographs of polished vertical-transverse sections of AA6063 FSW welds made using various parameters. The micrographs are taken at (a) 10x and (b) 20x magnifications as shown in flowing figures.

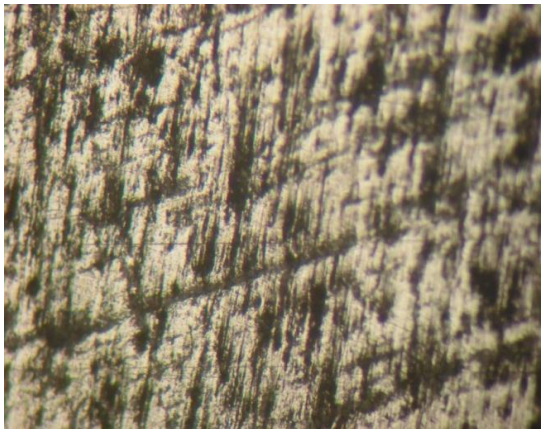

Fig5.66(a): for specimen no 1

Fig66(b)

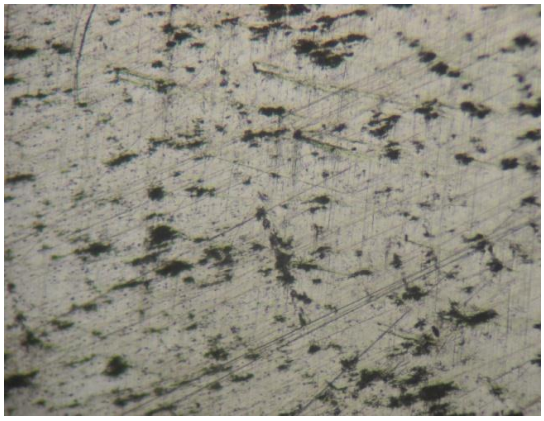

Fig5.67(a): for specimen no 2

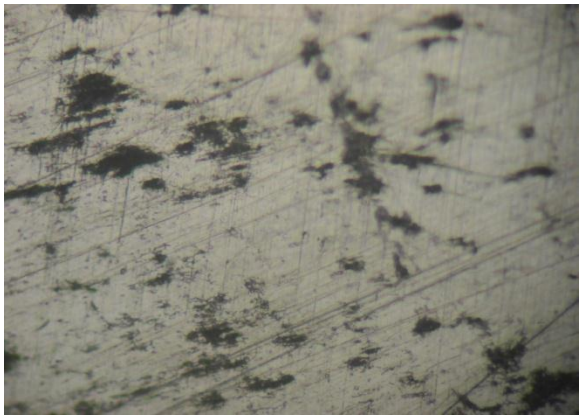

Fig67(b)

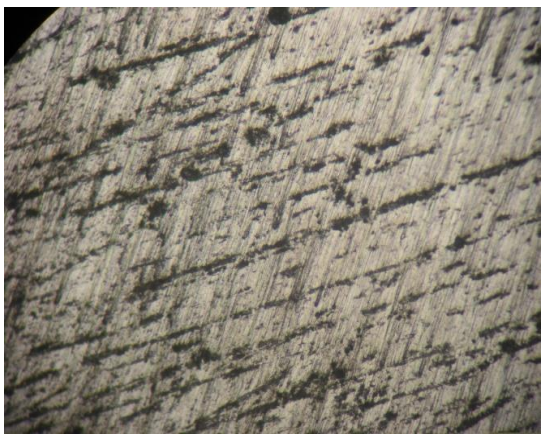

Fig5.68(a): for specimen no 3

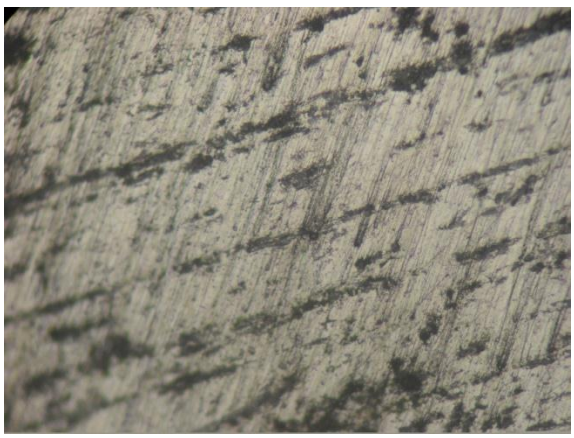

Fig68(b)

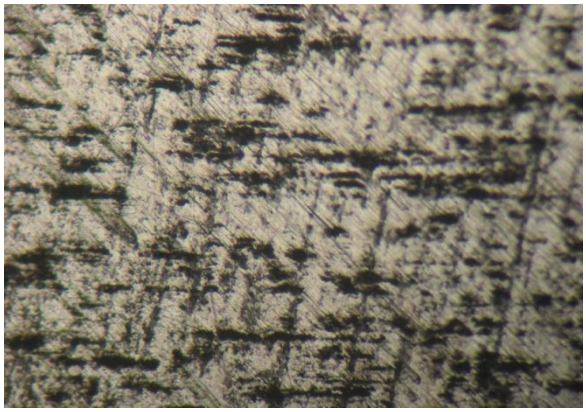

Fig5.69(a): for specimen no 4

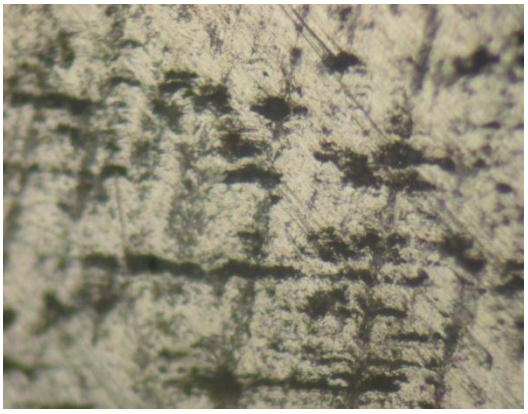

Fig5.69(b)

Fig5.70(a): for specimen no 5

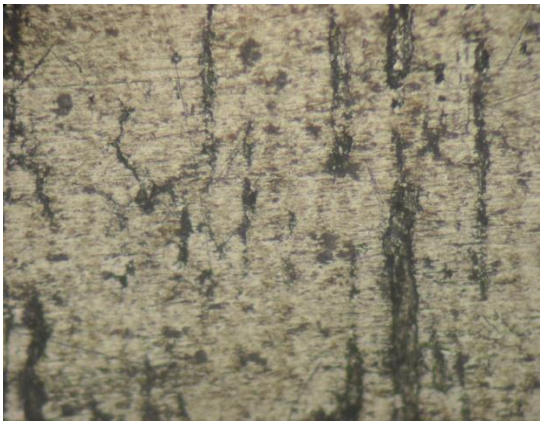

Fig5.70(b)

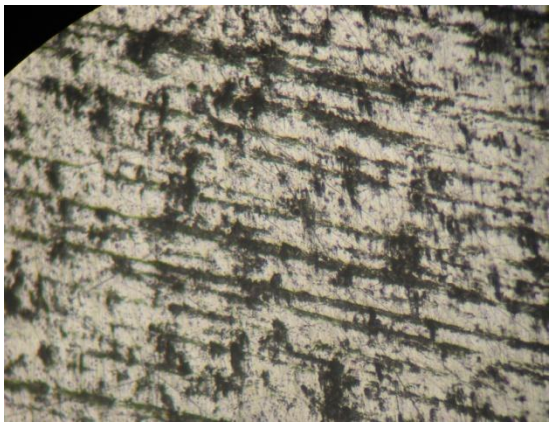

Fig5.71(a): for specimen no 6

Fig71(b)

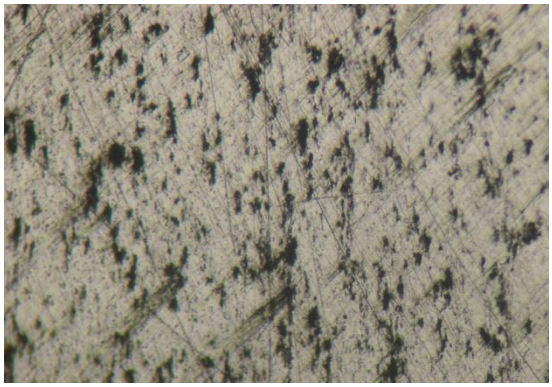

Fig5.72(a): for specimen no 7

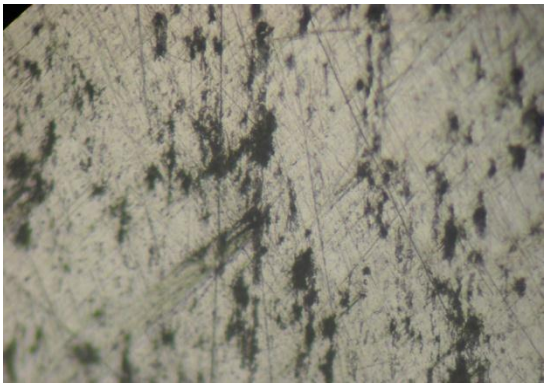

Fig72(b)

Fig5.73(a): for specimen no .8

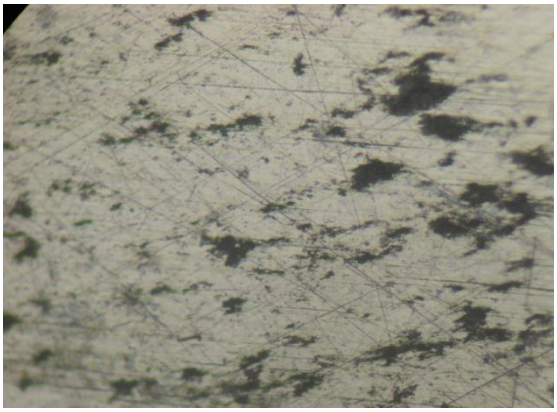

Fig73(b)

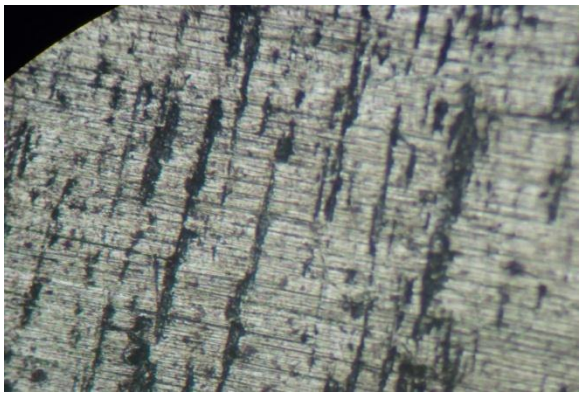

Fig5.74(a): for specimen no 9

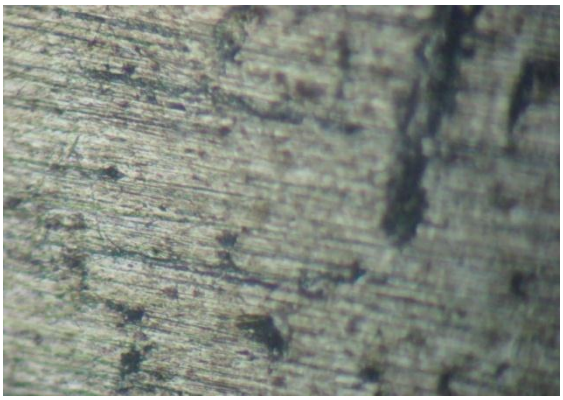

Fig74(b)

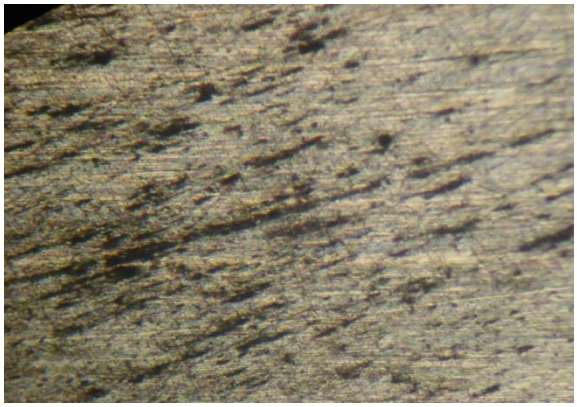

Fig5.75(a): for specimen no 10

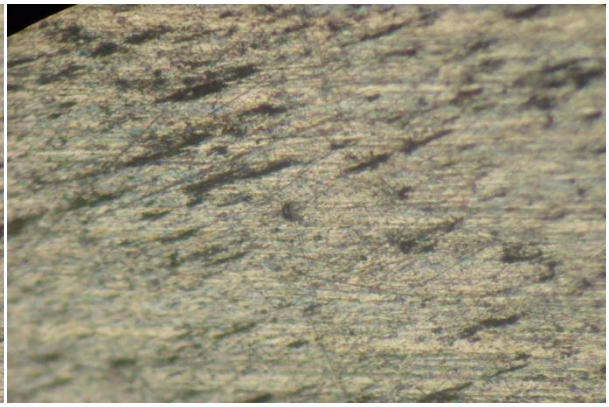

Fig75(b)

Fig5.76(a): for specimen no 11

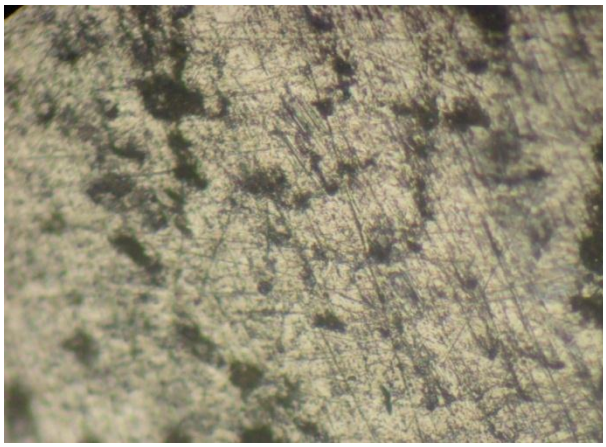

Fig76(b)

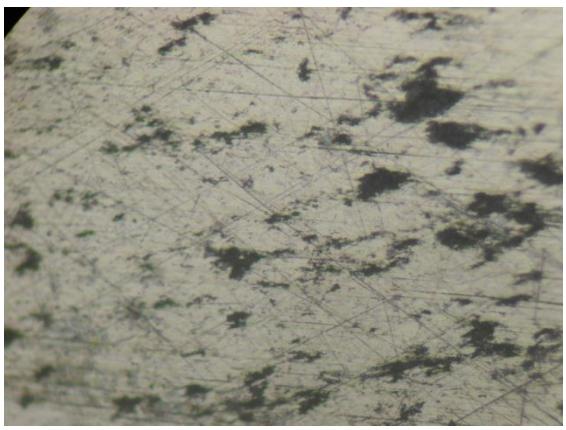

Fig5.77(a): for specimen no 12

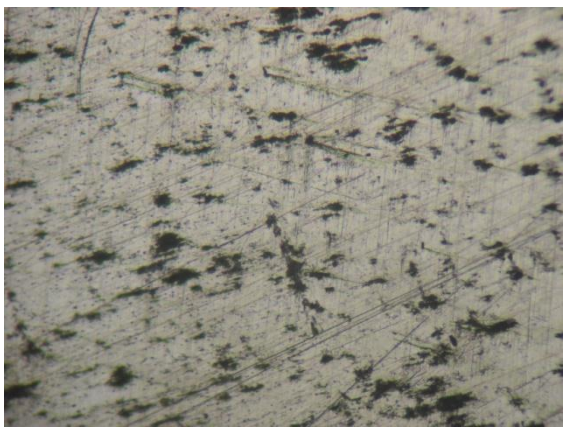

Fig77(b)

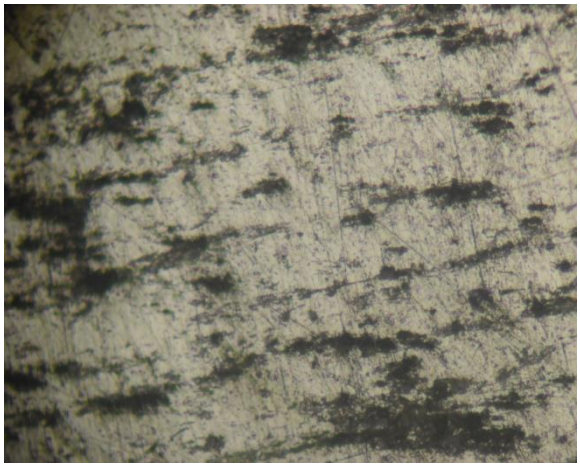

Fig5.78(a): for specimen no 13

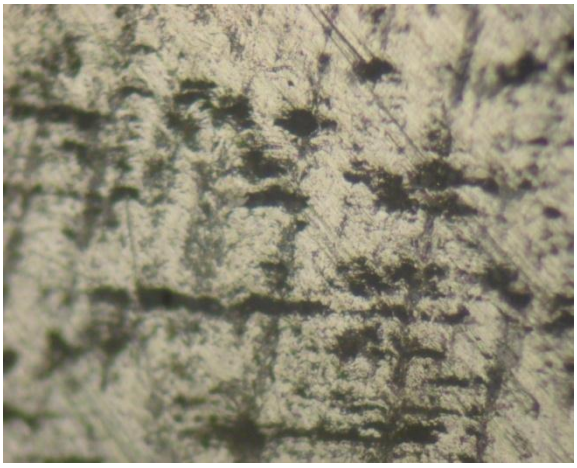

Fig78(b)

Fig5.79(a): for specimen no 14

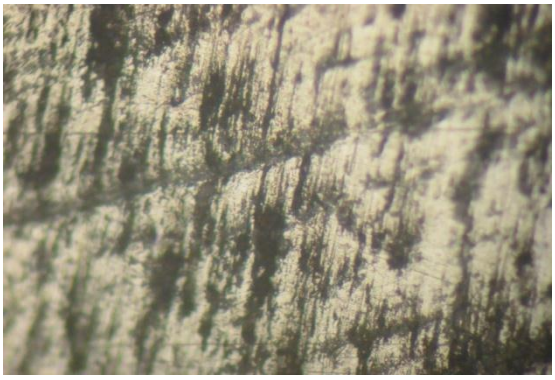

Fig79(b)

Fig5.80(a): for specimen no 15

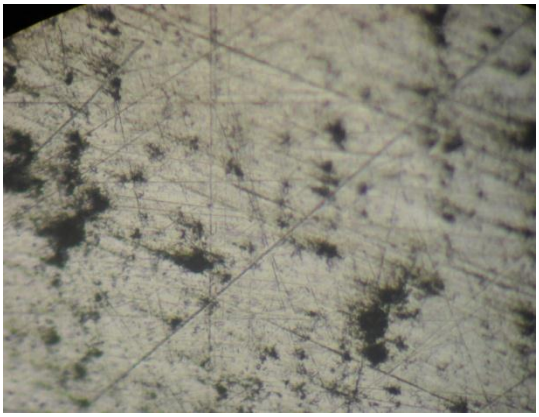

Fig5.80(b)

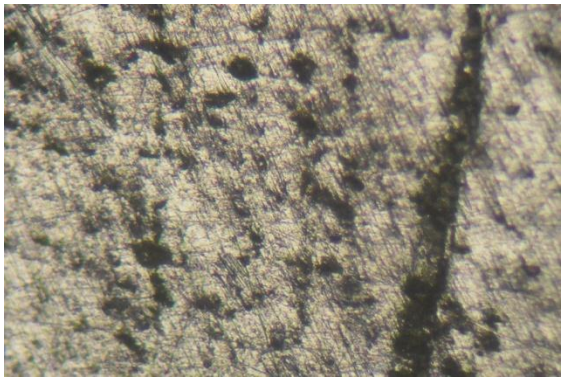

Fig5.81(a): for specimen no 16

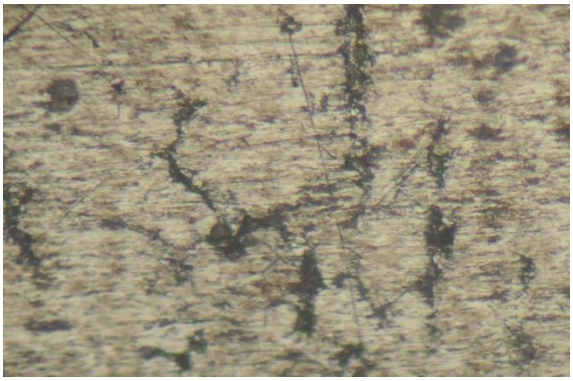

Fig5.81(b)

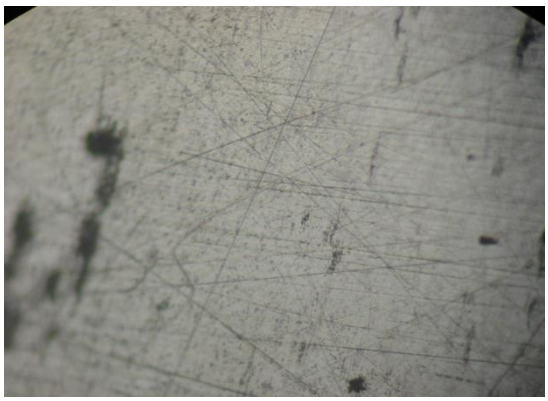

Fig5.82(a): for Base material

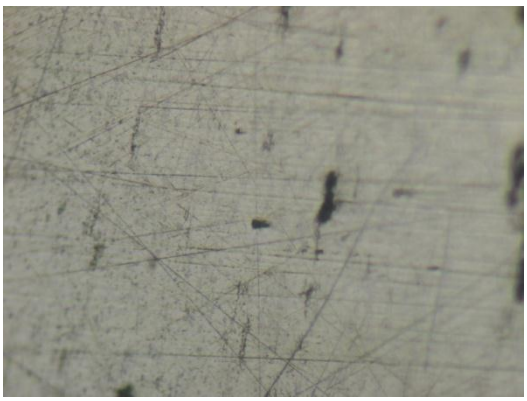

Fig5.82(b)

5.6.1 Discussion on Microstructure

The microstructure and consequent other properties produced during friction stir welding of aluminium alloys are dependent on several factors. Some of the contributing factors include alloy composition, alloy temper, gage of plate weld and welding parameters

Alloy composition determines the available strengthening mechanisms and how the material will be affected by the temperature during welding

The alloy temperature determines the starting microstructure, which can have an important effect on the alloy response to FSW, particularly in the heat-affected zone (HAZ).

Plate gage and welding parameters (e.g. tool rotational speed and welding speed) may affect the temperature distribution within the weld zone.

CHAPTER 6
CONCLUSIONS

AA6063 plates were successfully welded; some of the following conclusions were drawn on the behalf of graphs and tabled obtained.

- A minimum pin size was required to produce a weld. Pins that were too small in diameter i.e. 1 mm could not produce a weld. Pin diameter from 2 to 4 mm showed good joint tensile strength.
- Tensile strength is higher with lower weld speed and higher rotational speed; this indicates that lower range of weld speed is suitable for achieving maximum tensile strength.
- Rockwell hardness of the weld metal is lower than that of the parent metal; therefore the weld metal is weaker than the parent metal.
- Higher surface finish is obtained at high rotational speed and low tool traverse speed.
- Alignment of workpiece welding line and tool is an important factor to be considered to obtain sound weld and good mechanical properties.
- No filler metals and external source of heat (arc, gas) was used while performing the experiment, hence no exhaustible resources are involved.

CHAPTER 7

FUTURE OUTLOOK FOR FSW

- Other than pure aluminium all series of aluminium alloy which can't be welded by any other process can be welded by FSW using different combinations of plate thickness and welding speed. Pure aluminium can't be friction stir welded due to its high thermal conductivity and low melting point.
- Dissimilar friction stir welding can be done i.e. two different materials can be welded like aluminum alloy and magnesium alloy. Other materials that can be also be used are zinc, copper, titanium, stainless steel.
- Aluminium metal matrix composites can be stir welded since there is no melting during FSW, problems associated with liquid-solid reactions are eliminated , this makes FSW a potential process for joining Al-MMC's
- Effect of different tool geometries can be made like- convex shoulder, truncated cone pin; flat bottom cylindrical pin on mechanical and micro structural properties can be evaluated.
- Different tool materials can also be used, like tungsten carbide tool for welding aluminium silicon alloy and tool with PCBN pin to stir weld stainless steel.
- Other parameters like- welding plate thickness, tool tilt angle, plunge depth can be varied to see the variations.
- FSW can also be performed with a standard industrial robot on aluminium upto 3mm thickness.

REFERENCES

[1] W.M Thomas ,E.D .Nicholas, J.C. Needham, M.G. Murth; 'Friction stir butt welding' International Patent Application No PCT/GB92/02203, Dec 1991.

[2] R.S.Mishra and M.W.Mahoney; 'Friction stir welding and processing' Doi; 10.136/ fswp , 2007

[3] M.Peel, A.Steuwer, M.Preuss,P.JWithers; 'Microstructure, mechanical properties and residual stresses as a function of welding speed in aluminium AA5083 friction stir welds',6th International Symposium on FSW 2006.

[4] G.Cam, 'Recent developments in friction stir welding' Makina Tek.120, Pg48-58, 2007

[5] J. Adamowski, C. Gambaro, E. Lertora, M. Ponte, M. Szkodo; 'Analysis of FSW weld made od aluminium alloy AW6082-T6' Int.Scientific Journal Vol 28, Pg-453-460 August 2007.

[6] A. Lanciotti, and F. Vitali; 'Characterization of friction stir welded joints in aluminium alloy 6082-T6 plates', Welding International,Pg-624-630, August 2007

[7] K.N.Krishna; 'Formation of onion rings in Friction stir welds' Mater.Sci Eng .A, Vol 327,Pg-246-251,2002.

[8] www.en.wikipedia.org/wiki/Friction_stir_welding

[9] Prado, RA; Murr, LE; Shindo, DJ; Soto; 'Tool wear in the friction stir welding of aluminium alloy 6061+20% Al2O3':Apreliminary study". Scripta Materialia ,Pg-75 80. doi:10.1016/S1359-6462(01)00994-0, 2001

[10]Murr, LE. Liu, G; McClure; 'Dynamic recrystallisation in the friction-stir welding of aluminium alloy' Journal of materials Science Letters , doi:10.1023/A:1018556332357, 1997

[11] A.P. Reynolds and W.D. Lockwood, 'Digital Image Correlation for Determination

of Weld and Base Metal Constitutive Behavior', Proceedings of the First International Conference on Friction Stir Welding, June, 1999.

[12] T.W. Nelson, H. Zhang, and T. Haynes, 'Friction Stir Welding of Aluminum MMC 6061-Boron Carbide, Proceedings of the Second International Conference on Friction Stir Welding, June, 2000.

[13] K. Colligan, 'Dynamic Material Deformation During Friction Stir Welding of Aluminum, Proceedings of the Second International Conference on Friction Stir Welding', June, 2000

[14] M. Collier, R. Steel, T. Nelson, C. Sorensen, and S. Packer; 'Grade Development of Polycrystalline Cubic Boron Nitride for Friction Stir Processing of Ferrous Alloys', Proceedings of the Fourth International Conference on Friction Stir Welding, May, 2003

[15] T.J. Lienert, W.L. Stellwag, Jr., B.B. Grimmett, and R.W. Warke; 'Friction stir welding Studies on Mild Steel, Weld. ', Pg-1-s to 9-s Jan 2003

[16] R. Rai, H. K. D. H. Bhadeshia and T. DebRoy; 'Friction stir welding tools', Science and technology of welding and joining, Vol 16, Doi10.1179/1362171811Y.0000000023, Jan 2011

[17] R. Nandan, G. G. Roy, T. J. Lienert, and T. DebRoy; 'Numerical modelling of 3d plastic flow and heat transfer during friction stir welding of stainless steel' Science and Technology of Welding and Joining, Pg-526–537, 2006

[18] S. Brinckmann, A. von Strombeck, C. Schilling, J.F. dos Santos, D. Lohwasser, and M. Koçak, 'Mechanical and Toughness Properties of Robotic-FSW Repair Welds in 6061-T6 Aluminum Alloys', Proceedings of the Second International Conference on Friction Stir Welding, June 26–28, 2000

[19] O. Frigaard, O. Grong, and O. T. Midling; 'A process model for friction stir welding of age hardening aluminium alloys. Metallurgical & Materials Transactions', pg-1189–1200, 2001

[20] E.DNicholas;'Developments in the friction-stir welding of metals'. ICAA-6: 6th International Conference on aluminium alloys, 1998.

[21] Fred Delany, Stephan W Kallee, Mike J Russell; 'Friction stir welding of aluminium ships', International Forum on Welding Technologies in the Shipping Industry (IFWT), June 2007.

[22] Friction Stir Welding Demonstrated for Combat Vehicle Construction for 2519 aluminum armor for the U.S. Marine Corps' Advanced Amphibious Assault Vehicle and Welding Journal 03 2003

[23] A. Barcellona, G. Buffa, L. Fratini and D. Palmeri; 'Micro structural phenomena occurring in friction stir welding of aluminium alloys', Journal of Materials Processing Technology, Volume 177, Issues 1-3, , Pg- 340-343, 3 July 2006.

[24] Ahmed Khalid Hussain and Syed Azam Pashan Quadri; 'Parameters of friction stir welding od AA6351 Aluminium alloy', International Journal of Engineering Science and Technology, Vol. 2(10), 5977-5984, Dec 2010.

[25] A.P. Reynolds, W.D. Lockwood, and T.U. Seidel, Processing-Property Correlation in Friction Stir Welds, Mater.Sci.Forun, Vol 331-337,2000, Pg-1719-1724.

[26] G. Cam, S. Gucluer, A. Cakan, H.T. Serindag; 'Mechanical properties of friction stir butt welded Al-5086 h32 plates', Materials science and engineering technology, doi: 10.1002/mawe.200800455, Aug 2009.

[27] G. Campanile, P. Cavaliere, F. Panella, A. Squillace; 'Effect of processing parameters on micro structural properties of AA6056 joints produced by Friction stir welding', Journal of materials processing technology, Vol:18, Pg-263-270, doi:10.1016/ /j.jmatprotec.2006.06.015, 2006

[28] G. R. Babu, K. G. K. Murti and G. Ranga Janardhana; ' An experimental study on the effect of welding parameters on mechanical and micro structural properties of AA 6082-T6 friction stir welded butt joints', ARPN Journal of engineering and applied sciences, Vol 3, Oct 2008.

[29] H. Schmidt, J. Hattel and J Wert; 'An analytical model for the heat generation in friction stir welding', Modelling and Simulation in Materials Science and Engineering, Vol: 12, Issue: 1, Pg-143-157, doi: 10.1088/0965-0393/12/1/013, 2004.

[30] H.J. Liu, H. Fuji, and K. Nogi; 'Analyze the friction stir welding characteristics of 2017-T351 aluminium alloy sheet', Frontiers in Automobile and Mechanical Engineering (FAME), doi: 10.1109/FAME.2010.5714839, 25-27 Nov. 2010 .

[31] J. Adamowski, M Szkodo; 'Properties and micro structural changes in friction stir welds in the AA6082-T6', Archives of Materials Science and Engineering, Vol 28, Issue 8, Pg- 453-460, August 2007.

[32] K. Elangovan, V. Balasubramanian, S. Babu; 'Mathematical model to predict tensile strength of the friction stir welded AA6061', Journal of Materials Engineering and Performance, doi:10.1007 / s11665-008-9240-6, 2008.

[33] K.Kimapong and T.Watanabe; 'Effects of pin rotational speed, position of the pin axis, and pin diameter on the tensile strength and microstructure of the joint', American Welding Society, Vol: 83, Issue: 10, Pg-277-282, 2004.

[34] Loureiro, C.A.Leitao; 'Effect of friction stir welding parameters on the microstructure and mechanical properties of welds in two automotive aluminium alloys', Vol51, Issue SPEC. ISS., Pg- 433-440, 15 July 2007.

[35] M. K. Kulekci, E. Kaluc and O.Basturk; 'Comparison of the mechanical properties of welded joints of 6061-T6 aluminium alloy obtained with friction stir welding(FSW) and conventional metal inert gas welding(MIG)', Arabian Journal for Science and Engineering, Vol 35, Pg- 1B, June 2009.

[36] M.K. Shivaraj and Vijay Dinakaran; 'Improvement in micro hardness and mechanical properties shown by aluminium alloys AA2024-T4 and AA7075-T6 after friction stir welding', 2nd International Conference ,doi: 10. 1109 /ICCET. 2010 .54853 31 , Pg- V5-1 - V5-5 , April 2010

[37] N.T. Kumbhar and K. Bhanumurthy; 'FSW trials using a vertical milling machine on aluminium 6061 alloy', Asian J. Exp. Sci., Vol. 22, No. 2, Pg- 63-74,2008.

[38] P. Cavaliere, E. Cerri and Squillace; 'Mechanical and micro structural properties of 2024 and 7075 aluminium alloys joined together by friction stir welding', Journal of Materials Science, Vol: 40, Issue: 14, Pg- 3669-3676, doi: 10.1007/s10853-005-0474-5, 2005.

[39] T.J. Lienert, W.L. Stellwag, B.B. Grimmett and R.W. Warke; 'Friction Stir Welding Studies on Mild Steel', Welding journal, Pg-1s,Jan 2003.

[40] T. Sakthivel and J. Mukhopadhyay; 'Microstructure and mechanical properties of friction stir welded copper', Journal of material science, Vol 19, Doi: 10.1007/s10853-007-1666-y, 2007

[41] Yan Qiu and Wen Zhang; 'Dissimilar friction stir welding between 5052 aluminum alloy and AZ31 magnesium alloy', Trans. Nonferrous met society China,pg-s619-s623,2010.

[42] W. David Kelton; 'Experimental design for simulation' Winter simulation Conference, Pg-40-44,2000